Available online at www.sciencedirect.com
SCIENCE DIRECT
Neural Networks 19 (2006) 354–374
Neural Networks
www.elsevier.com/locate/neunet

A neural network model of Parkinson's disease bradykinesia

Vassilis Cutsuridis [a,b,*], Stavros Perantonis [a]

[a] Computational Intelligence Laboratory, Institute of Informatics and Telecommunications, National Center for Scientific Research 'Demokritos', Agia Paraskevi, Athens GR-15310, Greece
[b] Department of Informatics and Telecommunications, National University of Athens, Panepistimiopolis, Ilissia, Athens GR-15784, Greece

Received 9 November 2004; accepted 11 August 2005

Abstract

Parkinson's disease (PD) is caused by dopamine (DA) depletion consequent to cell degeneration in the substantia nigra pars compacta (SNc) and the ventral tegmental area (VTA). Although computational analyses of PD have focused on DA depletion in DA-recipient parts of the basal ganglia, there is also extensive DAergic innervation of the frontal and parietal cortex as well as the spinal cord. To understand PD bradykinesia, a comprehensive network model is needed to study how patterns of DA depletion at key cellular sites in the basal ganglia, cortex and spinal cord contribute to disordered neuronal and spinal cord activity and other PD symptoms. We extend a basal ganglia-cortico-spinal circuit for control of voluntary arm movements by incorporating DAergic innervation of cells in the cortical and spinal components of the circuit. The resultant model simulates successfully several of the main reported effects of DA depletion on neuronal, electromyographic (EMG), and movement parameters of PD bradykinesia.

Keywords: Bradykinesia; Parkinson's disease; Dopamine; Cortex; Spinal cord; Basal ganglia; Reaction time; Movement time

1. Introduction

Bradykinesia is the hallmark and most disabling symptom of Parkinson's disease (PD). Early in the disease, the most notable manifestation of bradykinesia is difficulty with walking, speaking, or getting into and out of chairs (Gibberd, 1986). Individuals might fail to swing an arm during walking, or they maybe lacking of facial expression (Abbs, Hartman, & Vishwanat, 1987; Gibberd, 1986; Weiner & Singer, 1989). Later, the bradykinesia affects all movements and, at its worst, can result in a complete inability to move. Patients require intense concentration to overcome the apparent inertia of the limbs that exists for the simplest motor tasks. Movement initiation is particularly impaired when unnatural or novel movements are attempted (Connor & Abbs, 1991), or when combining several movements concurrently (Benecke, Rothwell, & Dick, 1986; Lazarus & Stelmach, 1992).

The causes of bradykinesia are not known, in part because there are multiple pathways from the sites of neuronal degeneration to the muscles. The most important pathways are: (1) the pathway from the substantia nigra pars compacta (SNc) and the ventral tegmental area (VTA) to the striatum and from the striatum to the substantia nigra pars reticulata (SNr) and the globus pallidus internal segment (GPi) and from there to the thalamus and the frontal cortex, (2) the pathway from the SNc and the VTA to the striatum and from the striatum to the SNr and the GPi and from there to the brainstem, and (3) the pathway from the SNc/VTA to cortical areas such as the supplementary motor area (SMA), the parietal cortex, and the primary motor cortex (M1), and from there to the spinal cord.

Abbreviations: DA, dopamine; MPTP, 1-methyl-4-phenyl-1,2,5,6-tetrahydropyridine; SNc, substantia nigra pars compacta; GPe, external segment of globus pallidus; GPi, internal segment of globus pallidus; D_1, dopamine receptor from family 1; D_2, dopamine receptor from family 2; VTA, ventral tegmental area; SNr, substantia nigra pars reticulata; SMA, supplementary motor area; M1, primary motor cortex; CPG, central pattern generators; SN, substantia nigra; RRA, retrorubral area; BG, basal ganglia; LED, light-emitting diodes; EMG, electromyographic signal; RT, reaction time; PD, Parkinson's disease; EMD, electromechanical delay; OM, onset of movement; STN, subthalamic nucleus; VLo, ventrolateral thalamus; SP, substance P; DYN, dynorphin; ENK, enkephalin; MT, movement time; VITE, vector-integration-to-endpoint; FLETE, factorization of length to tension; DV, difference vector activity; TPV, target position vector; PPV, present position vector; DVV, desired velocity vector; RO, reciprocal; UD, unidirectional; BD, bidirectional; CRT, cellular reaction time; PMT, premotor reaction time; ME, movement end; MN, motoneurons; IN, interneurons; γ-MN, gamma motoneurons; IbIN, spinal type Ib interneurons; IaIN, spinal type Ia interneurons; α-MN, alpha motoneuron.

* Corresponding author. Address: Computational Intelligence Laboratory, Institute of Informatics and Telecommunications, National Center for Scientific Research 'Demokritos', Agia Paraskevi, Athens GR-15310, Greece. Tel.: +30 210 6503140; fax: +30 2106532175.
E-mail address: vcut@iit.demokritos.qr (V. Cutsuridis).

0893-6080/$ - see front matter © 2005 Elsevier Ltd. All rights reserved.
doi:10.1016/j.neunet.2005.08.016

Nomenclature

G	GO signal	β_{I}	contraction rate
G_0	GO signal amplitude	Γ_{F}	force threshold
T	time	Θ	joint angle
$\Im$	onset of time	F_{e}	external force
β	free parameter	I_{m}	moment of inertia
$u[t]$	step function	η	viscosity coefficient
V_{i}	DV activity	E_{i}	stretch reflex
T_{i}	target position command	R_{i}	renshaw cell activity
A_{i}	current position command	z_{i}	renshaw cell recruitment rate
$\mathrm{DA}_{1,2,3,4,5,6,7,8}$	dopamine modulatory parameters	R_{i}^{+}	rectified renshaw cell activity
B_{u}	baseline activity of DVV cell	Z_{i}^{+}	rectified spinal inhibitory interneuron (IN) activity
u_{i}	DVV cell activity	Z_{i}	spinal inhibitory (IN) activity
P	co-contraction signal	M_i^{+}	rectified αMN activity
F_{i}	muscle force	I_{i}	spinal Ia IN activity
k	scaling parameter	I_{i}^{+}	rectified Ia IN activity
L_{i}	muscle length	X_{i}	spinal Ib IN activity
Γ_{I}	resting muscle length	Y_{i}	spinal inhibitory IN activity
C_{i}	muscle contractile state	S_{i}	static γ-MN activity
D_{i}	dynamic γ-MN activity	G_{s}	feedback gain signal
N_{i}	dynamic intrafusal muscle contraction	G_{v}	gain parameter
D_{i}^{+}	rectified dynamic γ-MN activity	$h(w)$	activation function
B_{i}	number of contractile fibers	S_{i}^{+}	rectified static γ-MN activity
W_{i}	spindle receptor activation	U_{i}	static intrafusal muscle contraction
M_{i}	alpha MN activity	$\mathrm{d}\Theta/\mathrm{d}t$	joint velocity
λ	scaling factor	γ	free parameter

The most popular view is that cortical motor centers are inadequately activated by excitatory circuits passing through the basal ganglia (BG) (Albin, Young, & Penney, 1989). As a result, inadequate facilitation is provided to motor neuron pools and hence movements are small and weak (Albin et al., 1989). The implication of this view is that cells in the cortex and spinal cord are functioning normally. This paper will suggest otherwise.

In this paper, we integrate experimental data on the anatomy, neurophysiology, and neurochemistry of the globus pallidus internal segment, the cortex and the spinal cord structures, as well as data on motor impairments in PD to extend a well established neural model of basal ganglia–cortex–spinal cord interactions during movement production (Bullock & Grossberg, 1988, 1989, 1991, 1992; Bullock & Contreras-Vidal, 1993; Contreras-Vidal, Grossberg, & Bullock, 1997; Bullock, Cisek, & Grossberg, 1998). Computer simulations will show that disruptions of the BG output and of the SNc's DA input to frontal and parietal cortices and spinal cord may be responsible for delayed movement initiation. The main hypothesis of the model is that elimination of DA modulation from the SNc disrupts, via several pathways, the build-up of the pattern of movement-related responses in the primary motor and parietal cortex, and results in a loss of directional specificity of reciprocal and bidirectional cells in the motor cortex as well as in a reduction in their activities and their rates of change. These changes result in delays in recruiting the appropriate level of muscle force sufficiently fast and in an inappropriate scaling of the dynamic muscle force to the movement parameters. A repetitive triphasic pattern of muscle activation is sometimes needed to complete the movement. All of these result in an increase of mean reaction time and a slowness of movement (i.e. bradykinesia).

2. Background

2.1. Dopamine innervation of primate neocortex and spinal cord

A widespread dopaminergic innervation of the primate neocortex and spinal cord is now known to exist (Bjorklund & Lindvall, 1984; Williams & Goldman-Rakic, 1998) and is commonly implicated in psychiatric and neurological disorders, such as Parkinson's disease and schizophrenia. The source of the dopaminergic fibers in neocortex are considered to be the neurons of the substantia nigra (SN), the VTA, and retrorubral area (RRA) (Williams & Goldman-Rakic, 1995). DA afferents are densest in the anterior cingulate (area 24) (Berger, Trottier, Verney, Gaspar, & Alvarez, 1988a,b,c; Elsworth, Deutch, Redmond, Sladek, & Roth, 1990; Williams & Goldman-Rakic, 1998) and the motor areas (areas 4, 6, and SMA) (Berger et al., 1988; Elsworth et al., 1990; Gaspar,

Duyckaerts, Alvarez, Javoy-Agid, & Berger, 1991; Gaspar, Stepniewska, & Kaas, 1992; Williams & Goldman-Rakic, 1998), where they display a tri-laminar pattern of distribution, predominating in layers I, IIIa, and V–VI. In the granular prefrontal (areas 46, 9, 10, 11, 12) (Gaspar et al., 1991, 1992; Scatton, Javoy-Agid, Rouquier, Dubois, & Agid, 1983), parietal (areas 1, 2, 3, 5, 7) (Lewis, Morrison, & Goldstein, 1988; Lidow, Goldman-Rakic, Gallager, Geschwind, & Rakic, 1989), temporal (areas 21, 22) (Berger et al., 1988a,b,c), and posterior cingulate (area 23) (Berger et al., 1988) cortices, DA afferents are less dense and show a bilaminar pattern of distribution in the depth of layers I, and V–VI. The lowest density is in area 17, where the DA afferents are mostly restricted to layer I (Berger et al., 1988).

In addition to the dopaminergic innervation of the neocortex, the presence of dopaminergic fibers in the spinal cord has been observed by several groups (Bjorklund & Skagerberg, 1979; Blessing & Chalmers, 1979; Takada, Li, & Hattori, 1988). These dopaminergic fibers are predominately localized in the superficial layers, the laminae III–V of the dorsal horn, and in lamina X. These dopaminergic fibers arise from the posterior and dorsal hypothalamic areas and the periventricular gray matter of the caudal thalamus. Recent evidence (Weil-Fugazza & Godefroy, 1993) have demonstrated the occurrence of a dopaminergic innervation of the ventral horn (layers VII and VIII, and lamina IX). Dopamine receptors D_1 and to a lesser extent, D_2, are found in the dorsal as well as in the ventral spinal cord (Dubois, Savasta, Curet, & Scatton, 1986). The source of the ventral dopaminergic innervation is the caudal hypothalamus A11 cell group (Shirouzou, Anraku, Iwashita, & Yoshida, 1990).

It has also been shown that the dopaminergic fibers in the spinal cord might in part be projections of neurons from the substantia nigra (Commissiong, Gentleman, & Neff, 1979). Unilateral lesion of the substantia nigra produced by the injection of 6-hydroxydopamine (6-OHDA) significantly reduced the DA content in the striatum and the spinal cord on the side of the injection. This observation suggests the existence of an uncrossed nigrospinal dopaminergic pathway. However, no such input to the spinal cord has been demonstrated by anatomical methods.

An excellent review of the many dopaminergic systems and their cortical and spinal projections is Bjorklund & Lindvall (1984). A schematic diagram of the dopaminergic innervation of the basal ganglia (BG) and sensory-motor cortex is depicted in Fig. 1.

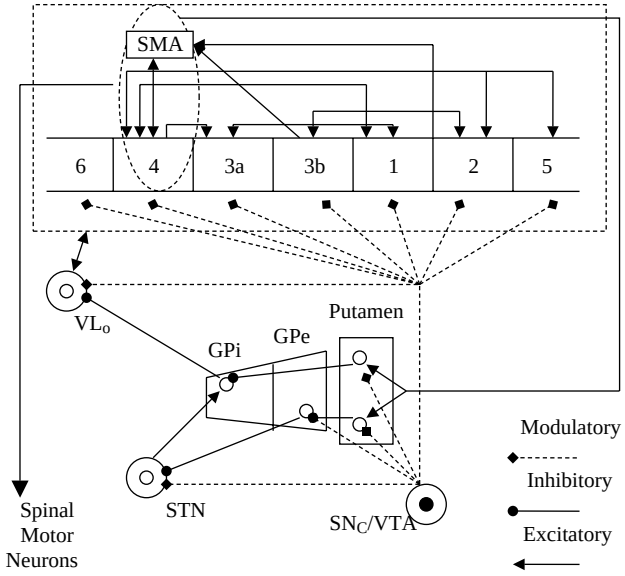

Fig. 1. Schematic diagram of dopaminergic innervation of basal ganglia and sensory-motor cortex. Arrow-ending solid lines, excitatory projections; Dot-ending solid lines, inhibitory projections; Diamond-ending dotted lines, dopamine (DA) modulatory projections; STN, subthalamic nucleus; GP_i, globus pallidus internal segment; GP_e, globus pallidus external segment; VL_o, ventrolateral thalamus; SNc, substantia nigra pars compacta; VTA, ventral tegmental area; SMA, supplementaty motor area; 1, 2, 3a, 3b, 4, 5, 6, Brodmann cortical areas 1, 2, 3a, 3b, 4, 5, 6, respectively.

2.2. Prior models

2.2.1. Contreras-Vidal and Stelmach model

Contreras-Vidal & Stelmach (1995) proposed a detailed model of basal ganglia-thalamocortical relations in normal and parkinsonian movements (Contreras-Vidal, 1999). The model's architecture was based on the 'direct' and 'indirect' pathways schema of the basal ganglia. In this model, the cortical input was shared by a pair of neighboring putamen output neurons. In the putamen, competitive interactions via feedback surround inhibition performed contrast enhancement and noise suppression of the cortical inputs. The putamen output projections formed distinct parallel pathways (direct and indirect pathway) to the GPi. The direct pathway led to an inhibition of the GPi cells, whereas the indirect pathway resulted in the activation of the GPi neurons via the inhibitory indirect pathway through the external segment of the globus pallidus (GPe) and the excitatory pathway through the subthalamic nucleus (STN). The GPi acted as a normally closed gate that could have been transiently opened by phasically activating the direct pathway and closed by activating the indirect pathway. Opening the gate through inhibition of GPi caused disinhibition of the motor thalamus (VLo), which activated the same cortical areas that produced the striatal activation. In the model, an opponent neurochemical differentiation such as the existence of GABA, substance P (SP), and dynorphin (DYN) in the direct pathway and GABA and enkephalin (ENK) in the indirect pathway was modeled in order to reflect the differential neurochemical and neurophysiological disturbances due to dopamine (DA) depletion. Moreover, most striatal cells projecting to GPi expressed the D_1 dopamine (DA) receptor, whereas those projecting to GPe expressed mainly the D_2 DA receptor. The model predicted that akinesia and bradykinesia did not result from malfunction of independent basal ganglia processes, but rather that these features of Parkinson's disease (PD) formed a continuum that went from normal reaction time (RT) and movement time (MT) to delayed RT and prolonged MT, and finally akinesia.

2.2.2. Brown, Bullock and Grossberg model

Brown, Bullock, and Grossberg (2004) advanced a comprehensive neural network model of saccadic eye movements in various experimental conditions (fixation, saccade, overlap, gap, and delayed tasks). Although the model was designed to satisfy the staging requirements of conditional voluntary behavior by exploring how the BG interact with laminar circuits in the frontal cortex and superior colliculus, a detailed BG model was formulated. According to this model, the basal ganglia structures contextually gate expression of reactive plans. Plan execution is released by activation of the direct pathway. In contrast with other models (Berns & Senjowski, 1995; Contreras-Vidal, 1999; Taylor & Taylor, 2000), competition for plan expression is mediated by activation of striatal GABAergic inhibitory interneurons and not by recurrent inhibition of striatal excitatory neurons. The model also proposed that the indirect pathway activation enabled deferral (STOP signal) of a chosen plan and the thalamo-striatal feedback signal guided learning of the indirect pathway's deferral responses.

3. Methods

3.1. Network structure

Fig. 2 schematizes the components of basal ganglio-cortico-spinal network model. As a basal ganglio-cortical network, we chose the VITE (Vector Integration To End point) model of Bullock & Grossberg (1988), which we here extend. The original VITE model was chosen because (1) it is capable of generating single joint arm movements (Bullock & Grossberg, 1988), and (2) it permits the functional interpretation and simulation of properties of many types of identified cortical neurons (Bullock et al., 1998).

In our version of the VITE model (Bullock & Grossberg, 1988, 1989, 1991, 1992), the types and properties of the cortically identified neurons are extended and the effects of dopamine depletion on key cortical cellular sites are studied. In the model, an arm movement difference vector (DV) is computed in parietal area 5 from a comparison of a target position vector (TPV) with a representation of the current position called perceived position vector (PPV). The DV signal then projects to area 4, where a desired velocity vector (DVV) and a non-specific co-contractive signal (P) (Humphrey & Reed, 1983) are formed. A voluntarily scalable GO signal multiplies (i.e. gates) the DV input to both the DVV and P in area 4, and thus volitional-sensitive velocity and non-specific co-contractive commands are generated, which activate the lower spinal centers. The DVV and P signals correspond to two partly independent neuronal systems with the motor cortex. DVV represents the activity of reciprocal neurons (Doudet, Gross, Arluison, & Bioulac, 1990), and it is organized for the reciprocal activation of antagonist muscles. P represents the activity of bidirectional neurons (i.e. neurons whose activity decreases or increases for both directions of movement (Doudet et al., 1990)), and it is organized for the co-contraction of antagonist muscles. Whereas the reciprocal pattern of muscle activation serves to move the joint from an initial to a final position, the antagonist co-contraction serves to increase the apparent mechanical stiffness of the joint, thus fixing its posture or stabilizing its course of movement in the presence of external force perturbations (Bullock & Contreras-Vidal, 1993; Humphrey & Reed, 1983).

The spinal recipient of our VITE variant model commands is the FLETE (Factorization of LEngth and Tension) model (Bullock & Contreras-Vidal, 1993; Bullock & Grossberg, 1989, 1991, 1992). Briefly, the FLETE model is an opponent processing muscle control model of how spinal circuits afford independent voluntary control of joint stiffness and joint position. It incorporates second-order dynamics, which play a large role in realistic limb movements. We extend the original FLETE model by incorporating the effect of the now cortically controlled co-contractive signal (in the original FLETE model, the co-contraction signal was simply a parameter) onto its spinal elements. Also, we study the effects that dopamine depletion on key spinal centers has on voluntary movements.

3.2. Mathematical formalism

We need to mention that most of the Eqs. (1, 6, 7, 8–12, 14,15, 17–31) presented in this section have been developed before by several other researchers (Bullock & Contreras-Vidal, 1993; Bullock & Grossberg, 1988, 1989, 1991, 1992; Bullock et al., 1998; Contreras-Vidal et al., 1997). Some of the Eqs. (2, 5, 13,16) are altered to incorporate the effects of dopamine, whereas new ones are also introduced Eqs. (3 and 4). In order to improve the readability of this section and help the readers of the paper, we list in this section all the equations (new and old) of the model.

In the model, the output of the BG system, the activity of the GPi (Horak & Anderson, 1984) is modeled by the GO signal

$$G(t) = G_0(t-\Im_i)^2 u[t-\Im_i]/(\beta + \gamma(t-\Im_i)^2) \quad (1)$$

where G_0 scales the GO signal, $(_i$ is the onset time of the ith volitional command, β and γ are free parameters, and $u[t]$ is a step function that jumps from 0 to 1 to initiate movement. Area 5 phasic cell activity (Chapman, Spidalieri, & Lamarre, 1984; Kalaska, Cohen, Prud'Homme, & Hyde, 1990), represented by the difference vector (DV), is described by

$$\frac{dV_i}{dt} = 30(-V_i + T_i - DA_1 A_i) \quad (2)$$

where T_i is the target position command, A_i is the current limb position command and DA_1 is the modulatory effect of dopamine on area 4′s PPV inputs to DV cell activity. Dopamine's values can range from 0 (lesioned) to 1 (normal) (Figs. 3 and 4).

The desired velocity vector (DVV), which represents area's 4 reciprocally activated cell activity (Doudet et al., 1990; Georgopoulos, Kalaska, Caminiti, & Massey, 1982; Kalaska, Cohen, Hyde, & Prud'Homme, 1989), is defined by

$$u_i = \left[G(DA_2 V_i - DA_3 V_j) + \frac{B_u}{DA_4}\right]^+ \quad (3)$$

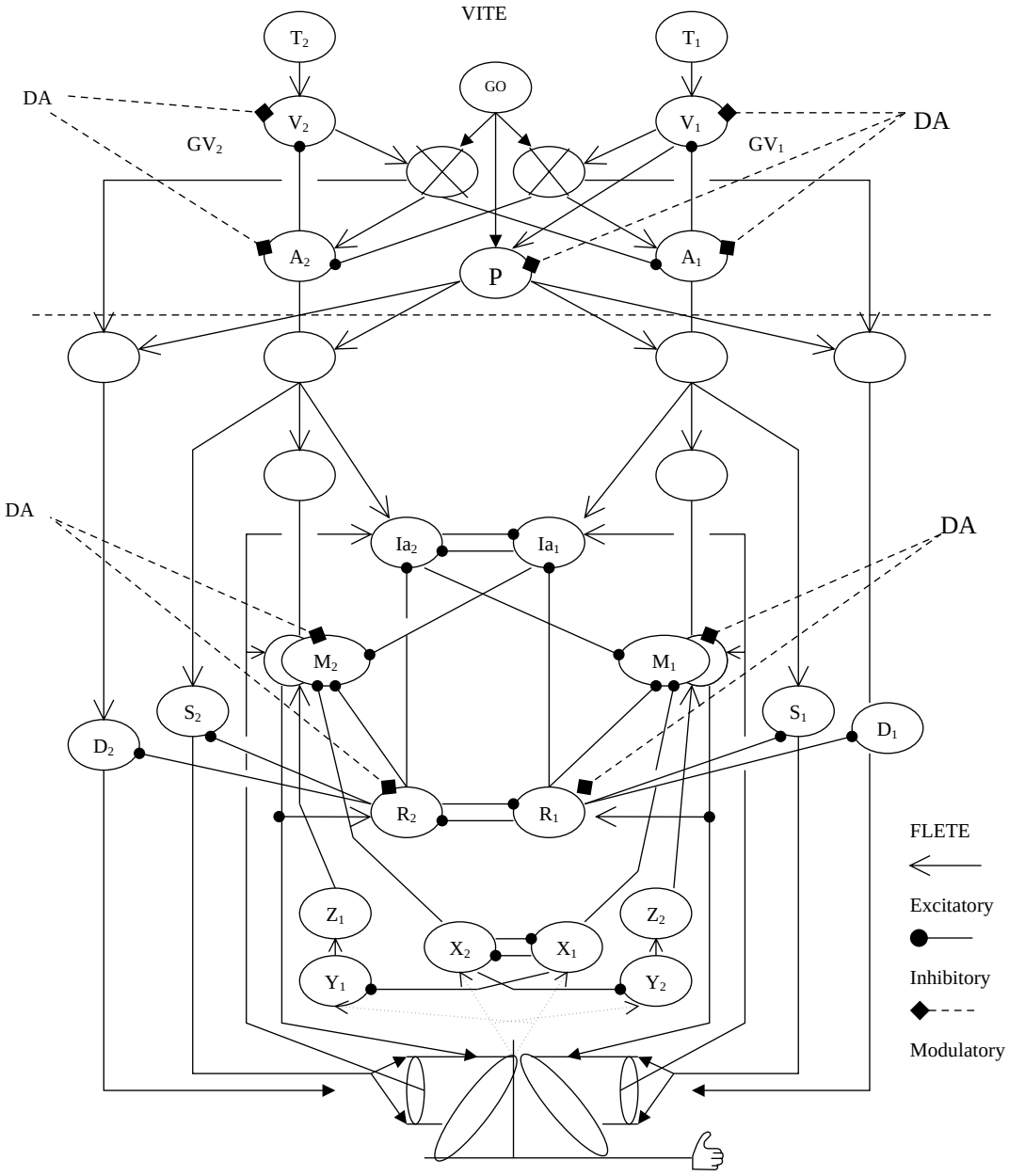

Fig. 2. Neural network representation of the cortico-spinal control system. (Top) The VITE model for variable-speed trajectory generation. (Bottom) the FLETE model of the opponent processing spinomuscular system. Arrow lines, excitatory projections; solid-dot lines, inhibitory projections; diamond dashed lines, dopamine modulatory inputs; dotted arrow lines, feedback pathways from sensors embedded in muscles; DA, dopamine modulatory signal; GO, basal ganglia output signal; P, bi-directional co-contractive signal; T, target position command; V, DV activity; GV, DVV activity; A, current position command; M, alpha motoneuronal (MN) activity; R, renshaw cell activity; X, Y, Z, spinal inhibitory interneuron (IN) activities; Ia, spinal type a inhibitory IN activity; S, static gamma MN activity; D, dynamic gamma MN activity; 1,2, antagonist cell pair.

where *i, j* designate opponent neural commands, B_u is the baseline activity of the phasic-MT area 4 cell activity, and DA_2, DA_3, are the modulatory effects of dopamine on DV inputs to DVV cell activity and DA_4 is the effect of dopamine on DVV baseline activity. Note from Eq. (3) that DV flexion (V_i) cell is modulated by a different DA parameter (DA_2) from the DV extension (V_j) cell (DA_3). As the reader can see from Table 1, in the normal case the values of $DA_{2,3} = 1$, whereas in the dopamine-depleted case the value of DA_2 is smaller than the value of DA_3. The later model assumption is supported by the experimental observations of Doudet et al. (1990) (Figs. 5 and 6) and Watts & Mandir (1992) (column 1 of Fig. 7). Briefly in both studies, normal and MPTP-treated monkeys were trained to make fast ballistic flexion and extension movements of the forearm, while their primary motor cortical and EMG activities were recorded. One of their findings was that the discharge frequency of flexion and extension reciprocal (RO) cells is reduced (compare RO activities in normal (column 1 of Fig. 5A and B) and MPTP (column 1 of Fig. 6A and B) cases) (Doudet et al., 1990). It is

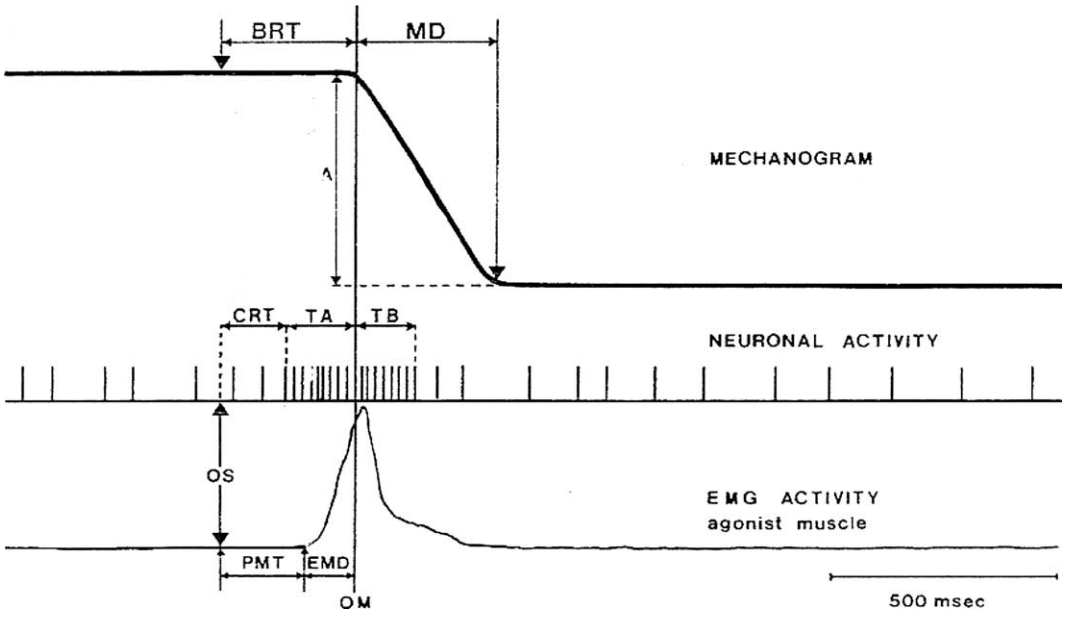

Fig. 3. Schematic representation of the parameters studied. Movement parameters (upper diagram), behavioral reaction time (BRT in ms); movement duration (MD in ms), movement amplitude (A in d°); Neuronal activity parameters (middle diagram), cellular reaction time (CRT in ms); duration (ms) of burst discharge preceding (Ta) and following (Tb) the onset of movement (OM) represented by the vertical line. EMG activity parameters (lower diagram), premotor time (PMT in ms) and electromechanical delay (EMD in ms) (reproduced with permission from Doudet et al., 1990, Fig. 1, p. 179, Copyright© 1990 Springer-Verlag).

clear from these figures that the firing intensity of the flexion cells is affected (reduced) more than the firing intensity of the extension cells.

Area 4 bidirectional neuronal activity (P) is represented by

$$P = \left[G(\mathrm{DA}_2 V_i - \mathrm{DA}_3 V_j) + \frac{B_P}{\mathrm{DA}_4}\right]^+ \tag{4}$$

Note that in Eqs. (3) and (4) parameters DA_2 and DA_3 attenuate the activities of the DV flexion and extension cells, respectively, whereas the parameter DA_4 facilitates the baseline activity of the DVV Eq. (3) and P Eq. (4) cells. These assumptions were strictly based on experimental observations (Doudet et al., 1990; Watts & Mandir, 1992; Gross, Feger, Seal, Haramburu, & Bioulac, 1983), which show that there is an overall reduction in the firing intensity of primary motor cortical cells (DVV and P signals) (see Section 4.1 and Figs. 5 and 6) and an increase in the baseline activity (see Fig. 7 and Section 4.1) post-MPTP.

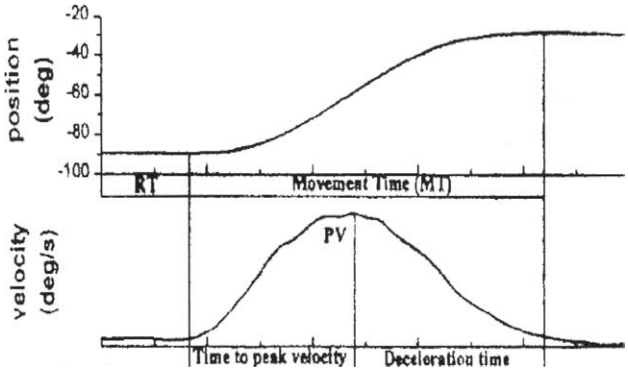

Fig. 4. Position and velocity traces of a young normal subject's elbow movement are shown. The following kinematic and time variables are displayed: reaction time (RT), movement time (MT), peak velocity (PV), time-to-peak velocity (TPV), deceleration time (DT) (reproduced with permission from Weiss et al., 1996, Fig. 1, p. 220, Copyright© 1996 Elsevier Science Ltd).

Area 4 tonic cell activity (Fromm, Wise, & Evarts, 1984; Kalaska et al., 1989), represented by the present position vector (PPV) dynamics is defined by

$$\frac{\mathrm{d}A_i}{\mathrm{d}t} = G[\mathrm{DA}_2 V_i]^+ - G[\mathrm{DA}_3 V_j]^+ \tag{5}$$

The quadratic force-length relationship of muscle is approximated by

$$F_i = k([L_i - \Gamma_i + C_i]^+)^2 \tag{6}$$

where k is a scaling parameter, F_i is muscle force, L_i is muscle length, Γ_i is resting muscle length, C_i is muscle contractile state and indices $i=\{1,2\}$ designate antagonist muscle pairs. The contractile state dynamics is defined by

$$\frac{\mathrm{d}C_i}{\mathrm{d}t} = \beta_i[(B_i - C_i)M_i - C_i] - [F_i - \Gamma_F]^+ \tag{7}$$

where Γ_F is the force threshold, M_i is the alpha-motoneuron (α-MN) pool activity in muscle control channel i, β_i is the contractile rate, and B_i is the number of contractile fibers recruited. The origin-to-insertion muscle lengths for opponent mono-articular muscles, which indicate that a change of joint angle always implies a length increment in one muscle and a length decrement in its opponent, are defined as

$$L_1 = \sqrt{(\cos\Theta)^2 + (20 - \sin\Theta)^2} \tag{8}$$

Table 1
Summary of model's output neuronal, muscular, and movement parameters for normal and dopamine-depleted conditions

	Normal	Dopamine depleted
CRT	3.04	3.08
T_A	10.08	14.84
T_B	3.64	21.13
PMT	0.024	0.026
EMD	13.10	17.90
RT	13.13	17.93
MT	18.45	60.43
TPV	3.62	4.51
DT	14.84	55.92
Peak DVV	0.18	0.12
Peak EMG	1.38	1.10
Peak velocity	0.14	0.11
Force	0.06	0.04

Units: time (ms). Normal parameter set, $G_0=0.6$, $\beta=100.5$, $\gamma=0.8$, $DA_{1-8}=1$; Dopamine-depleted parameter set, $G_0=0.2$, $\beta=100.5$, $\gamma=0.8$, $DA_1=0.9$, $DA_2=0.8$, $DA_3=0.9$, $DA_4=0.9$, $DA_5=0.95$, $DA_6=0.8$, $DA_7=0.8$, $DA_8=0.9$.

and

$$L_2 = \sqrt{(\cos\Theta)^2 + (20 + \sin\Theta)^2} \tag{9}$$

The limb dynamics for single joint movements is defined as

$$\frac{d^2\Theta}{dt^2} = \frac{F_1 - F_2 + F_e - \eta\frac{d\Theta}{dt})}{I_m} \tag{10}$$

where F_e is an external force, F_i is the muscle force of muscle i, $d\Theta/dt$ is the angular velocity in radians, I_m is the moment of inertia, and η is the joint viscosity coefficient. The contraction rate, which according to the size principle of motor unit organization (Henneman, 1957, 1985) depends on the level of excitatory input to the α-MN, is defined by

$$\beta_i = 0.05 + 0.01(A_i + P + E_i) \tag{11}$$

where A_i is the descending present position command, P is the coactivation signal, and E_i is the stretch feedback from the spindles. Likewise, the number of contractile fibers recruited into force production also depend on the net excitatory drive to the α-MN:

$$B_i = 0.3 + 3(A_i + P + E_i) \tag{12}$$

Renshaw population cell activity is modeled by

$$\frac{dR_i}{dt} = (5B_i - R_i)DA_5 z_i M_i - R_i(0.8 + DA_6 R_j) \tag{13}$$

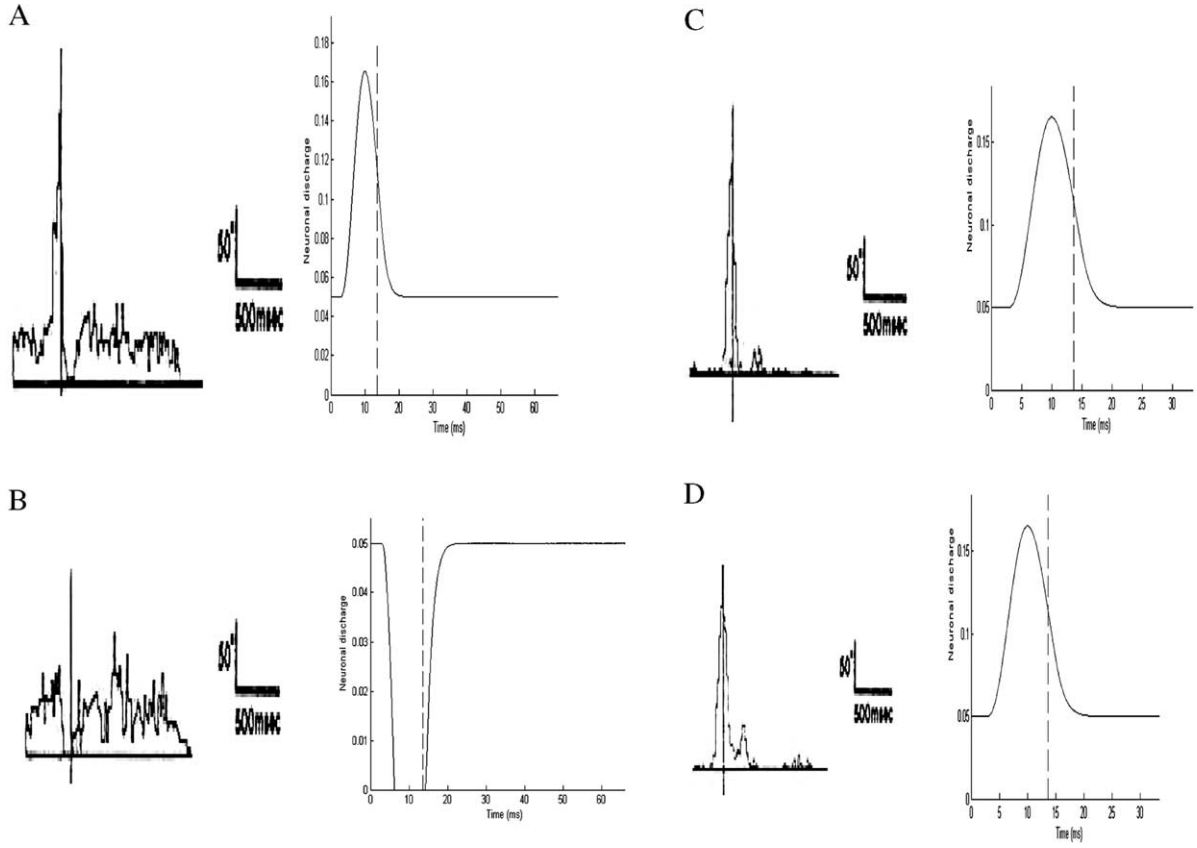

Fig. 5. Comparison of changes in the peristimulus time histograms (PSTH) of area's 4 reciprocally organized neurons (column 1; reproduced with permission from Doudet et al., 1990, Fig. 4A, p. 182, Copyright© Springer-Verlag), in simulated area's 4 reciprocally organized phasic (DVV) cell activities (column 2), in PSTH of area's 4 bidirectional neurons (column 3; reproduced with permission from Doudet et al., 1990, Fig. 4A, p. 182, Copyright© Springer-Verlag) and in simulated area's 4 co-contractive (P) cell activities (column 4) for a flexion (A and C) and extension (B and D) movements in a normal monkey. The vertical bars indicate the onset of movement. The spike discharges related to successive movements are accumulated into histograms, each bin corresponding to 10 ms. In the simulations, a GO signal of $G_0=0.6$, $\beta=100.5$, $\gamma=0.8$ and dopamine $DA_{1-8}=1$ (normal) were used. Note that 1 s of time is $\sim$100 time steps.

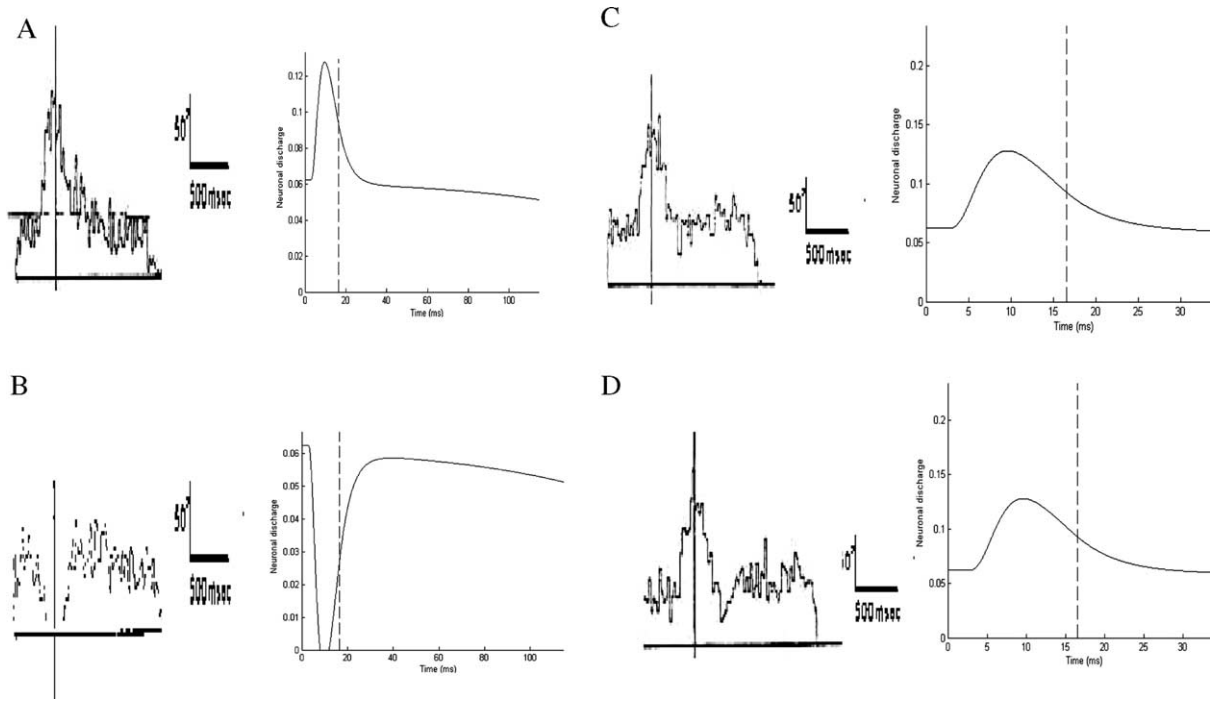

Fig. 6. Comparison of changes in the peristimulus time histograms (PSTH) of area's 4 reciprocally organized neurons (column 1; reproduced with permission from Doudet et al., 1990, Fig. 4B, p. 182, Copyright© Springer-Verlag), in simulated area's 4 reciprocally organized phasic (DVV) cell activities (column 2), in PSTH of area's 4 bidirectional neurons (column 3; reproduced with permission from Doudet et al., 1990, Fig. 4B, p. 182, Copyright© Springer-Verlag) and in simulated area's 4 co-contractive (P) cell activities (column 4) for flexion (A and C) and extension (B and D) movements in an MPTP-treated monkey. The vertical bars indicate the onset of movement. The spike discharges related to successive movements are accumulated into histograms, each bin corresponding to 10 ms. In the simulations, a GO signal of $G_0=0.1$, $\beta=120.5$, $\gamma=0.7$ and dopamine $DA_1=0.9$, $DA_2=0.7$, $DA_3=0.8$, $DA_4=0.8$, $DA_5=0.9$, $DA_6=0.8$, $DA_7=0.8$, $DA_8=0.9$ (MPTP-treated) were used. Note that 1 s of time is $\sim$100 time steps.

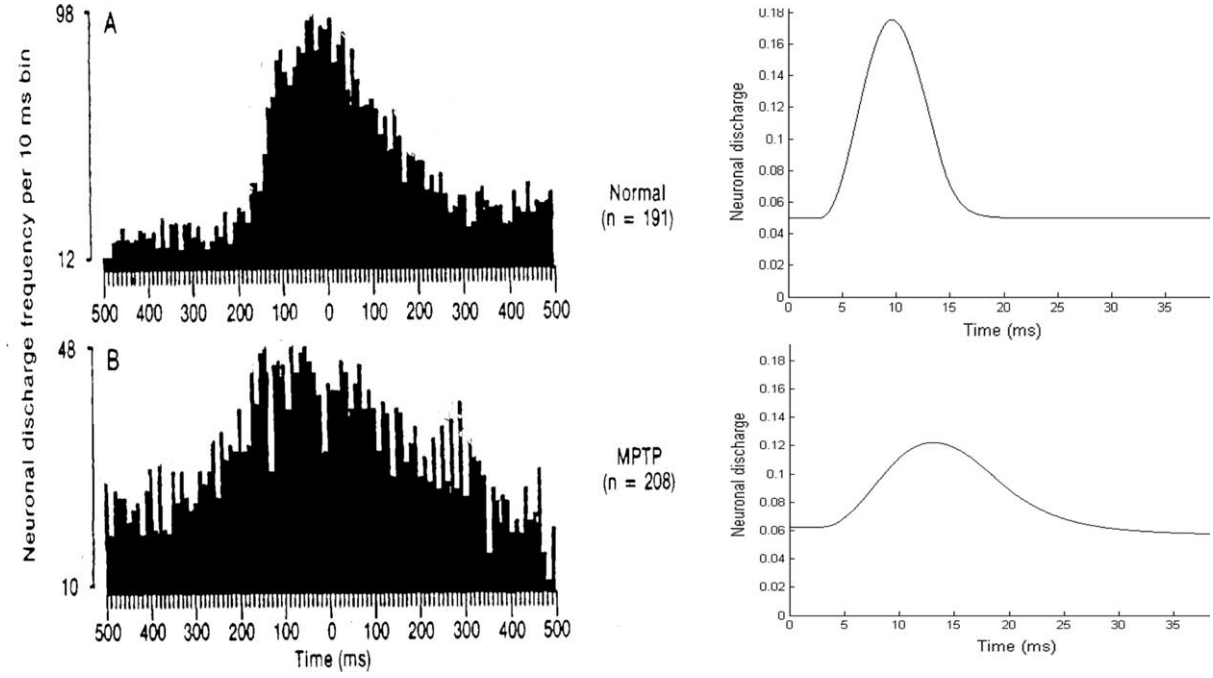

Fig. 7. (A) Comparison of peristimulus histograms (PSTH) of monkey primary motor cortex task-related neuronal activity (column 1) (reproduced with permission from Watts & Mandir, 1992, Fig. 7, p. 461, Copyright© Elsevier Science Ltd.) and simulated area's 4 phasic-MT cell activity (column 2) in normal state. (B) Comparison of peristimulus histograms (PSTH) of monkey primary motor cortex task-related neuronal activity (column 1) (reproduced with permission from Watts & Mandir, 1992, Fig. 7, p. 461, Copyright© Elsevier Science Ltd.) and simulated area's 4 phasic-MT cell activity (column 2) in MPTP state. The *y*-axes represent the number of spikes in a time bin of 10 ms. The *x*-axes represent time in ms. Note, in the hemiparkinsonian (MPTP) state, an overall reduction of firing intensity, an increase in baseline activity and a reduced rate of change of neuronal discharge.

where the Renshaw cell recruitment rate z_i is:

$$z_i = 0.05(1 + M_i) \tag{14}$$

and it depends on the level of α-MN activation. The Renshaw population output signal is

$$R_i^+ = \max(0, R_i) \tag{15}$$

which equals to R_i, as $R_i \geq 0$. The α-MN population activity is described by the following equation

$$\frac{dM_i}{dt} = (\lambda B_i - M_i)\mathrm{DA}_7\left(A_i + P + E_i + Z_j^+\right) - (M_i + 1.6)\mathrm{DA}_8\left(0.2 + R_i + X_i + I_j^+\right) \tag{16}$$

where X_i is the type Ib interneuron (IbIN) force feedback and Z_j is a signal dependent on the rate of change of IbIN force feedback in the opponent muscle channel. The α-MN population output signal is

$$M_i^+ = \max(0, M_i) \tag{17}$$

The type Ia interneuron (IaIN) population activity is defined as

$$\frac{dI_i}{dt} = (10 - I_i)(A_i + P + E_i) - (I_i + 1)\left(1 + R_i + I_j^+\right) \tag{18}$$

and its output signal is

$$I_i^+ = \max(0, I_i) \tag{19}$$

The IbIN population activity is excited by pathways originating in force-sensitive Golgi tendon organs

$$\frac{dX_i}{dt} = 0.2(5 - X_i)F_i - X_i(0.8 + 0.2X_j) \tag{20}$$

Two other Golgi tendon organ feedback-related activities are defined

$$\frac{dY_i}{dt} = 0.2(5 - Y_i)F_i - Y_i(1 + X_i) \tag{21}$$

$$\frac{dZ_i}{dt} = 0.2(5 - Z_i)Y_i - Z_i \tag{22}$$

This population's output signal is

$$Z_i^+ = \max(0, Z_i - 0.2) \tag{23}$$

The static γ-MN activity is described by

$$\frac{dS_i}{dt} = 5(2 - S_i)(A_i + P) - (S_i + 1.2)[0.2 + 0.3h(R_i)] \tag{24}$$

where $h(w) = w/(0.3 + w)$, and its output signal is

$$S_i^+ = \max(0, S_i) \tag{25}$$

The intrafusal muscle contraction associated with static γ-MN activation is described by

$$\frac{dU_i}{dt} = (2 - U_i)S_i^+ - U_i \tag{26}$$

The dynamic γ-MN activity is

$$\frac{dD_i}{dt} = (8 - D_i)\left(100G[V_i]^+ + P\right) - (D_i + 1.2)\left(1 + 100G[V_j]^+ + 0.5h(R_i)\right) \tag{27}$$

and its output signal is

$$D_i^+ = \max(0, D_i) \tag{28}$$

The intrafusal muscle contraction associated with dynamic γ-MN activation is

$$\frac{dN_i}{dt} = 0.1(2 - N_i)D_i^+ - 10N_i \tag{29}$$

The spindle receptor activation was defined as

$$\frac{dW_i}{dt} = (2 - W_i)([U_i + L_i - \Gamma_i]^+) + G_v\left(\left[N_i + \frac{dL_i}{dt}\right]\right)^+ - 10W_i \tag{30}$$

The stretch feedback signal is given by

$$E_i = G_s W_i \tag{31}$$

where G_s is the feedback gain signal. Note that in Eqs. (18, 20, 24–29) there is no DA. Although the effects of DA depletion in Ia (Bathien & Rondot, 1977; Obeso, Quesada, Artieda, & Martinez-Lage, 1985), Ib (Delwaide, Pepin, & Maertens de Noordhout, 1991; McCrea, 1992) and static and dynamic γ-MNs activities (Hagbarth, Wallin, Lofstedt, & Aquilonius, 1975) have been extensively studied, evidence seem to indicate that spinal Ia and Ib inhibitory interneurons play a role in PD rigidity (Delwaide et al., 1991; Obeso et al., 1985), whereas γ-MNs play a role in PD tremor (Hagbarth et al., 1975; Young, 1984). Whether rigidity and tremor contributes to bradykinesia is unclear. It has been reported that rigidity, tremor and bradykinesia occur independently (Jankovic, 1987). For these reasons, we limit the scope of our paper to only PD bradykinesia.

3.3. Implementation

The simulations were performed on a Pentium IV 3.2 GHz PC with MATLAB's version R13 installed. The whole system of differential and algebraic equations was implemented in MATLAB (The MathWorks, Inc, Natick, MA). Differential equations were integrated numerically using one of the MATLAB ordinary differential equation solvers (mainly ode45, an implicit solver based on the Dormand-Prince pair method (Dormand & Prince, 1980)) with time step $\Delta t = 0.001$ ms. Relative (error) tolerance was set to 10^{-4}.

The parameters for the normal functioning basal ganglio-cortico-spinal network used in the simulations are: $G_0 = 0.6$, $k = 1$, $\eta = 0.18$, $I_m = 1$, $\lambda = 0.95$, $T_1 = 1.4$, $T_2 = 0.3$, $G_i = 20.9$, $G_v = 2$, $G_s = 1$, $G_f = 1$, $\gamma = 1$, $\beta = 15.5$, $\mathrm{DA}_{1-8} = 1$ (Bullock et al., 1998; Contreras-Vidal et al., 1997).

4. Simulation results

4.1. Dopamine depletion effects on the task-related discharge patterns of cells in the primary motor cortex

Fig. 5 shows a qualitative comparison of cortical neuronal profiles (column 1 of Fig. 5A–D; Doudet et al. (1990)) and model cell responses (column 2 of Fig. 5–D) in area 4 for flexion, extension, and co-contraction in normal monkey during a simple voluntary reaching task (see Section 3.2 for a detailed description of the experimental study of Doudet et al. (1990)). A reciprocal organization of cellular activity is reported (column 1 of Fig. 5A and B). Similarly, the activity of bidirectional neurons tuned to both directions of movement is also shown (column 1 of Fig. 5C and D). The model is able to simulate successfully the activities of both reciprocal (DVV activity) cellular activity and bidirectional neurons (co-contraction signal, P) (column 2 of Fig. 5A–D).

In other studies, Watts & Mandir (1992) and Gross et al. (1983) examined the effects of MPTP-induced parkinsonism on the primary motor cortex task-related neuronal activity and motor behavior of monkeys when they were performing simple flexion and extension movements of the wrist and elbow, respectively. Watts & Mandir (1992) reported a decrease in peak discharge frequency, an increase in baseline activity and an increase in the latency between the start of M1 neuronal activity and movement onset and in the duration of after-discharge following movement onset in the hemi-parkinsonian state. Gross et al. (1983) observed a similar reduction of the maximal discharge frequency in lesioned animals compared to normal animals.

Fig. 6 shows qualitative simulations of reciprocally and bidirectionally activated neurons, when the output of the basal ganglia is reduced and cortical and spinal dopamine is depleted ($DA_1=0.9$, $DA_2=0.7$, $DA_3=0.8$, $DA_4=0.8$, $DA_5=0.9$, $DA_6=0.8$, $DA_7=0.8$, $DA_8=0.9$, $G_0=0.1$, $\beta=120.5$, $\gamma=0.7$; all other parameters values were the same as in normal case). Note that DA_1 parameter value is greater than the DA_2, DA_3 and DA_4 parameter values. As the reader might recall parameter DA_1 modulates the PPV input to area's 5 phasic (DV) cell activity (Eq. (2)), whereas parameters DA_2, DA_3 and DA_4 modulate the DV inputs to DVV and P cell activity (area's 4 RO and BD activities) and to DVV baseline activity (Eqs. (3) and (4)), respectively. As we mentioned in Section 2.1, DA afferents are densest in area 4 than they are in area 5. So, the effect of DA depletion would be stronger in area 4 than in area 5.

Also, in Fig. 6, notice an overall reduction of firing intensity (Doudet et al., 1990; Gross et al., 1983), a reduced rate of change of neuronal discharge (Doudet et al., 1990; Gross et al., 1983), a disorganization of neuronal activity (neuronal direction specificity is markedly reduced) (Doudet et al., 1990), and an increase in baseline activity (in normal case the baseline activity was 0.05, whereas in dopamine depleted the baseline activity increased to $\sim$0.07) (Doudet et al., 1990). Similar changes in neuronal activity including an increase in baseline activity are seen in Fig. 7 (Watts & Mandir, 1992).

Furthermore, there is an increased duration (see Table 1) in neuron discharge in area 4 preceding (T_A, in ms; Fig. 11) and following (T_B, in ms; Fig. 11) onset of movement (OM) resulting in a prolongation of its total response duration, exactly as it is observed in experimental studies (Benazzouz, Gross, Dupont, & Bioulac, 1992; Doudet et al., 1990; Gross et al., 1983; Watts & Mandir, 1992). In these model simulations, T_A was measured as the time interval between the first deviation of cellular discharge from the baseline activity till the onset of movement, whereas T_B was the time interval from the onset of movement till the time the neuronal activity returned to its baseline level (end of cellular discharge). A schematic representation of these time intervals is depicted in Fig. 3.

Fig. 8 shows a qualitative comparison of abnormal cellular responses of GPi neurons to striatal stimulation in MPTP-treated monkeys (Fig. 8A) (Tremblay, Filion, & Bedard, 1989) and simulated oscillatory GPi neuronal responses (Fig. 8B). In their study, Tremblay et al. (1989) failed to offer a functional role of such oscillatory responses. We propose that such GPi oscillatory responses (repetitive GO signal; Fig. 15A), comprising of at least two inhibitory–excitatory sequences

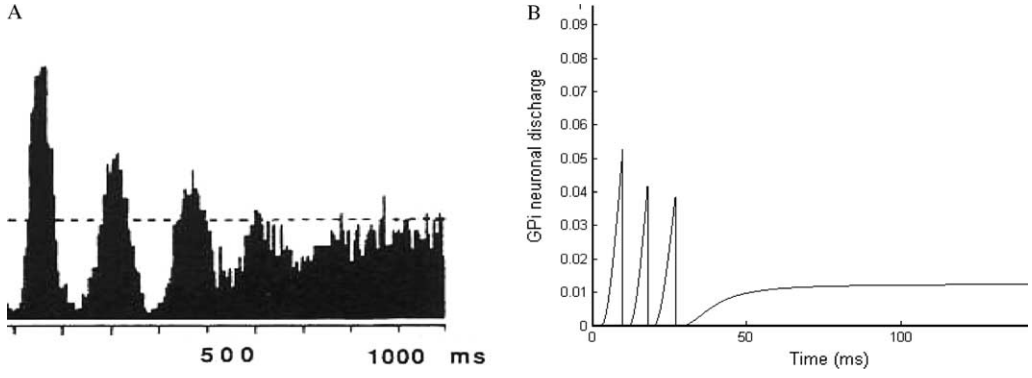

Fig. 8. Comparison of (A) peristimulus histograms (PSTH) of abnormal oscillatory responses of GPi neurons to striatal stimulation in MPTP-treated monkeys (reproduced with permission from Tremblay et al., 1989, Fig. 2, p. 23, Copyright© Elsevier Science Ltd), and (B) simulated oscillatory disrupted GPi responses. Note: oscillatory responses comprise of at least two inhibition–excitation sequences. Bin width is 6 ms. Parameter set: $G_0=0.15$, $\beta=100.5$, $\gamma=0.8$, $DA_{1,3,4,8}=0.9$, $DA_{2,6,7}=0.8$, $DA_5=1$, all other parameters did not change. Time units in ms.

(see beginning of second paragraph of section 'GPi neurons' and Figs. 2 and 6 in Tremblay et al., 1989 study), gate (multiply) the DV signal and generate repetitive volitional motor commands (DVV signals; not shown), which in turn generate repetitive agonist–antagonist muscle bursts (see Fig. 10) needed sometimes by PD patients to complete the full amplitude of the movement.

4.2. Dopamine depletion effects on EMG activity

In normal individuals, single ballistic movements at a joint are made with a single biphasic pattern of EMG activity in agonist and antagonist muscles (Berardelli, Dick, Rothwell, Day, & Marsden, 1986; Brown & Cooke, 1984, 1990a, 1990b; Ghez & Gordon, 1987a, 1987b, 1987c; Gottlieb, Latash,

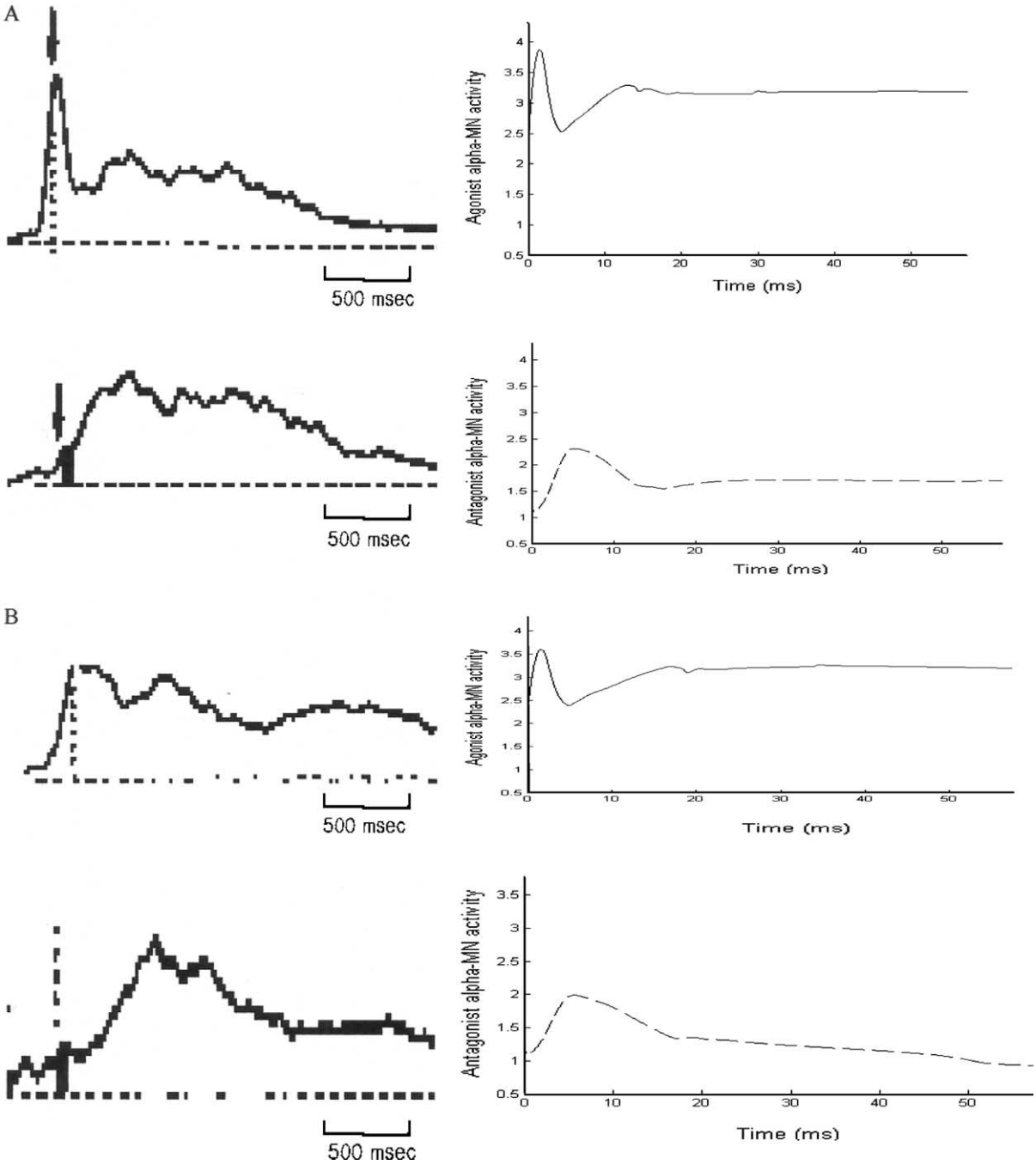

Fig. 9. (A) Comparison of electromyographic (EMG) (reproduced with permission from Godaux et al., 1992, Fig. 5, p. 97, Copyright© Wiley-Liss, Inc., a subsidiary of John Wiley & Sons, Inc) and simulated alpha motoneuronal (MN) activity for an agonist muscle (row 1) and antagonist muscle (row 2) in a normal movement. Arrow: onset of movement (OM). Time units in ms. (B) Comparison of electromyographic (EMG) (reproduced with permission from Godaux et al., 1992, Fig. 5, p. 97, Copyright© Wiley-Liss, Inc., a subsidiary of John Wiley & Sons, Inc) and simulated alpha motoneuronal (MN) activity for an agonist muscle (row 1) and antagonist muscle (row 2) in a Parkinson's disease (PD) movement. Dashed line: onset of movement (OM). Parameter set (PD condition): $G_0=0.2$, $\beta=100.5$, $\gamma=0.8$, $DA_{1,3,4,8}=0.9$, $DA_{2,6,7}=0.8$, $DA_5=0.95$. Time units in ms.

Corcos, Liubinskas, & Agarwal, 1992; Hallett & Marsden, 1979; Wierzbicka, Wiegner, & Shahani, 1986). The first agonist burst provides the impulsive force for the movement, whereas the antagonist activity provides the braking force to halt the limb. Sometimes a second agonist burst is needed to bring the limb to the final position. In bradykinetic patients with Parkinson's disease the size of the first agonist burst is reduced. Up to a certain size, movements might be performed relatively normally (Flowers (1976)), but there are times that movements would require additional bursts of EMG activity (Hallett & Khoshbin, 1980; Benazzouz et al., 1992; Doudet et al., 1990) in order for the limb to reach the target. The reason for such inappropriate scaling of the first agonist burst and for the repetitive triphasic pattern of muscle activation in Parkinson's disease movements is not known.

The model presented in this paper offers a plausible hypothesis of why PD EMG agonist burst activity is reduced and why on some occasions multiple agonist–antagonist–agonist bursts are needed to complete the movement. We propose that disruptions of GPi neuronal activity (BG output) and dopamine depletion in the cortex, shown earlier to disrupt the reciprocal organization of M1 neurons, reduce their activity, and increase their rate of change, as well as dopamine depletion in key cellular sites of the spinal cord result in the downscaling of the size of the first agonist burst and in the increase of its rate of change. So, in order for the subject to complete the movement and reach the target, additional EMG bursts are required (see Fig. 10).

Fig. 9 show a qualitative comparison of the normal (Fig. 9A) and dopamine depleted (Fig. 9B) simulated alpha motoneuronal (αMN) activities of the agonist (row 1) and antagonist (row 2) muscles and experimentally obtained muscle activations (Godaux, Koulischer, & Jacquy, 1992) in small amplitude movements. In their experimental paradigm, Godaux et al. (1992) tested the performance of control and PD subjects in a rapid button-pressing task, while they recorded their EMG activities. They reported a significant reduction in the peak agonist and antagonist amplitude as well as of their rate of development in patients with Parkinson's disease. In contrast to some PD studies (Benazzouz et al., 1992; Doudet, Gross, Lebrun-Grandie, & Bioulac, 1985; Hayashi et al, 1988) where co-contraction of agonist and antagonist muscles is reported, Godaux et al. (1992) clearly see a non-disrupted biphasic pattern of muscle activation (Fig. 9B). Several other human and animal studies have observed similar reductions of the rate of development and of the peak amplitude of the first agonist burst of EMG activity (Corcos, Chen, Quinn, McAuley, & Rothwell, 1996; Doudet et al., 1990; Hallett & Kalaska et al., 1989.; Watts & Mandir, 1992). Model simulations report similar reductions in the size of the agonist and antagonist bursts and their rate of change (column 2 of Fig. 9B; see also Table 1 for numerical value of peak agonist burst (EMG_{max}) in dopamine depleted case). A non-cocontractive agonist–antagonist pattern of muscle activation is also observed (column 2 of Fig. 9B). Furthermore, dopamine depletion has a small effect on premotor reaction time (from 0.0243 in normal case, it increased to 0.026 in DA lesioned case; see

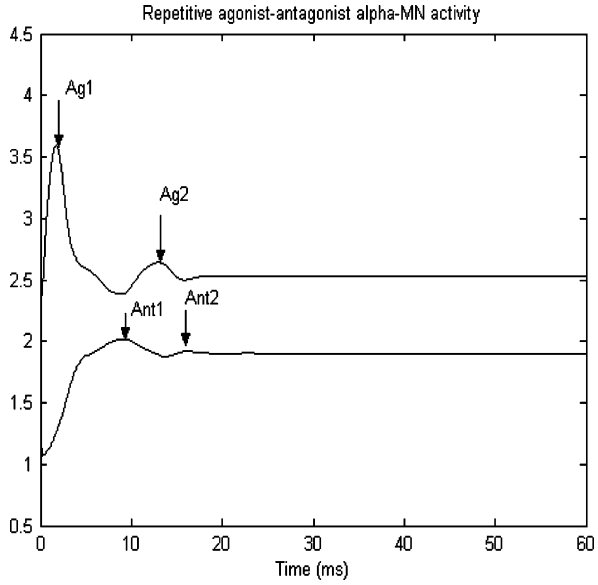

Fig. 10. Simulated repetitive biphasic alpha motoneuronal (MN) activity in a dopamine depleted movement. Vertical arrows indicate agonist–antagonist bursts needed to complete the movement. Each agonist–antagonist pair signifies a sub-movement. In this case, two agonist–antagonist pairs are required to complete the movement. An initial agonist (Ag1) and antagonist (Ant1) bursts to initiate it and an additional agonist (Ag2 < Ag1) and antagonist (Ant2 < Ant1) bursts to complete the full amplitude of movement.

Table 1) as it has been observed in Benazzouz et al. (1992) study, but increases considerably the electromechanical delay time (from 13.10 in normal case, it increased to 17.90 in DA depleted case; see Table 1) (Benazzouz et al., 1992; Doudet et al., 1990; Gross et al., 1983).

Fig. 10 shows the effect of the disrupted BG output (Fig. 15A) and of DA depletion in cortex and spinal cord in large amplitude movements, where a single biphasic agonist–antagonist muscle burst pattern is not sufficient to complete the movement. A repetitive biphasic pattern of muscle activation is clearly observed (indicated by the arrows) (Hallett & Khoshbin, 1980). Fig. 15A shows the depleted GO signal dynamics used to produce this repetitive EMG activity. As we explained in Section 4.1, the generation of such repetitive biphasic pattern of muscle activation is the result of the gating of the DV signal by multiple inhibition–excitation sequences of abnormal GPi activity (Fig. 8) for the generation of multiple volitional motor cortical commands sent down to the spinal cord for the completion of the movement.

4.3. Dopamine depletion effects on movement variables

Figs. 3 and 4 provide a schematic representation of the variables that will be presented in the section. We first provide some definitions of the movement variables: cellular reaction time (CRT) is the time from the beginning of the simulation to the change in neuronal activity; premotor reaction time (PMT) is the time elapsed from the beginning of the simulation to the beginning of the EMG activity in the agonist muscle; electromechanical delay (EMD) represents the duration of

the EMG activity in the agonist muscle before the onset of movement; reaction time (RT = PMT + EMD) is the time from the beginning of the simulation till the onset of movement; time-to-peak (TPV) is the time interval from the onset of movement till the time that corresponds to the peak velocity; movement time (MT) is the time from the onset of movement till the end of movement; deceleration time (DT) is the time interval from the time that corresponds to the peak velocity till the end of movement; peak velocity (V_{max}) is the maximum value of the velocity; peak EMG (EMG_{max}) activity is the maximum value of the EMG activity.

Fig. 11 shows a qualitative comparison of a forearm angular displacement (column 1; adapted from Gross et al., 1983) and a simulated position trace (column 2) centered on the onset of movement in normal (Fig. 11A) and dopamine depleted (Fig. 11B) cases. Movement onset and termination were estimated automatically with the use of the following algorithm (Teasdale, Philips, & Stelmach, 1993): (1) the maximum value of the velocity was found (V_{max}); (2) the sample at which the time series exceeds 10% of the V_{max} was located; (3) from this point back to the beginning of movement, the first sample, which was((0.1 V_{max} − 0.01 V_{max}) was searched and located; this was the onset sample. The end of the movement was determined by using the same algorithm as for the onset, but in reverse. In Fig. 11A and B, along with the position traces, horizontal histograms of cellular reaction time (CRT), neuronal time interval preceding onset of movement (T_A), time interval following onset of movement (T_B) and movement end (ME) depicted with the four vertical dashed lines are also displayed. In Fig. 11B, movements were still smooth, but both the RT (RT = CRT + T_A) and MT are significantly increased (Benazzouz et al., 1992; Camarata, Parker, Park, Haines, Turner and Chae, 1992; Doudet et al., 1990; Gross et al., 1983; Rand, Stelmach, & Bloedel, 2000; Watts & Mandir, 1992; Weiss, Stelmach, Adler, & Waterman, 1996) (see Table 1 for numerical values). While CRT is slightly affected by the dopamine depletion, T_A is markedly increased (Doudet et al., 1990; Gross et al., 1983).

Fig. 12 shows a qualitative comparison of experimentally obtained velocity profiles (column 1; adapted from Godaux

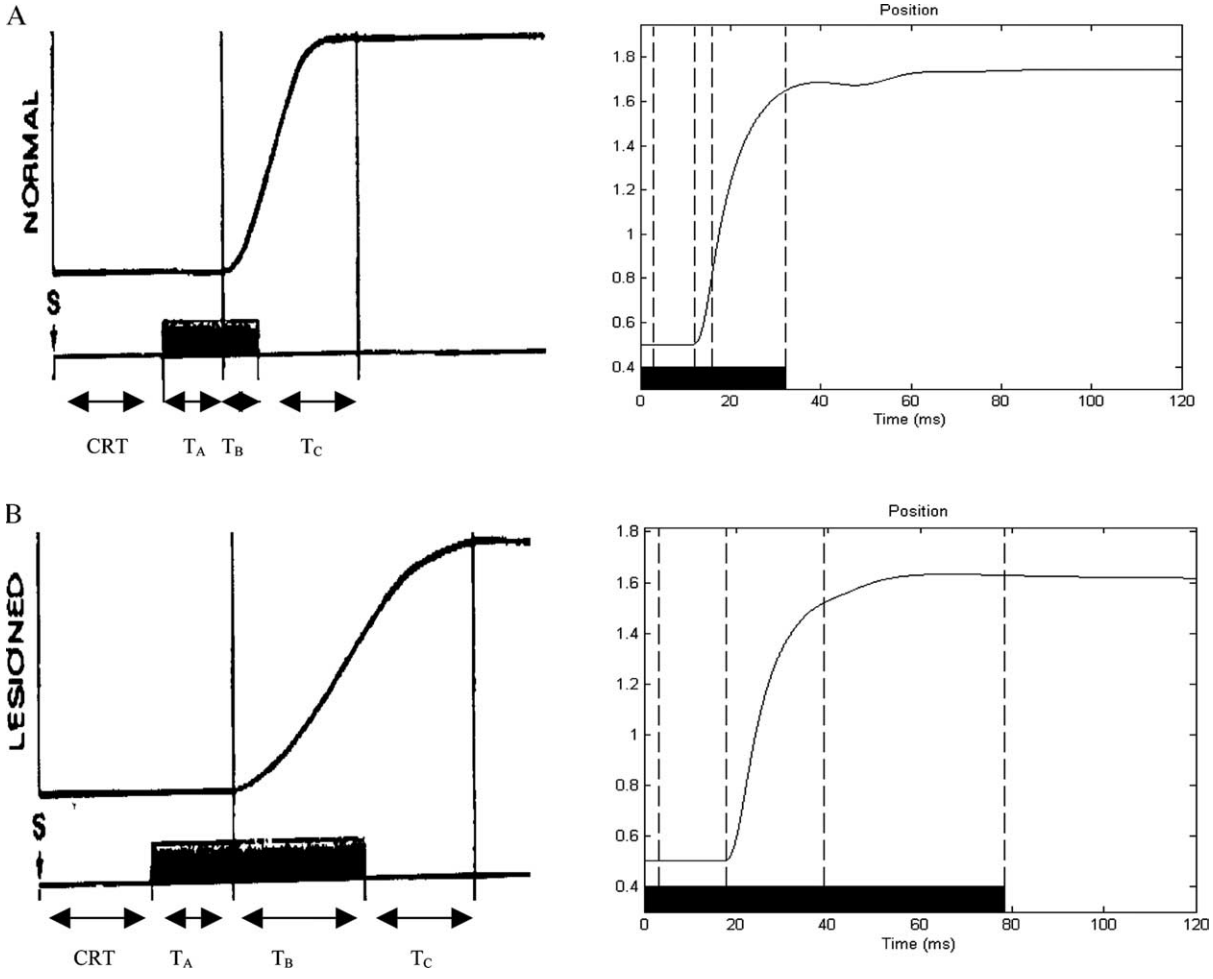

Fig. 11. Comparison of simulated (column 2) and experimentally obtained (column1; reproduced with permission from Gross et al., 1983, Fig. 5, p. 189, Copyright© Springer-Verlag) forearm displacement (position) in normal (A) and Parkinson's disease (B) conditions. Shaded area: representation of neuronal change related to movement. In A and B: (column 1) the vertical bar indicates the onset of forearm displacement; S, auditory cue; CRT, mean value of cellular reaction time; T_A, changes of neuronal activity preceding onset of movement (OM); T_B, changes of neuronal activity following OM; T_C, changes of neuronal activity from T_B till movement end (ME). (column 2) the time interval between vertical dashed lines starting from left to right indicate CRT, T_A, T_B, and T_C, respectively. Parameter set (PD condition): $G_0 = 0.2$, $\beta = 100.5$, $\gamma = 0.8$, $DA_{1,3,4,8} = 0.9$, $DA_{2,6,7} = 0.8$, $DA_5 = 0.95$.Time units in ms.

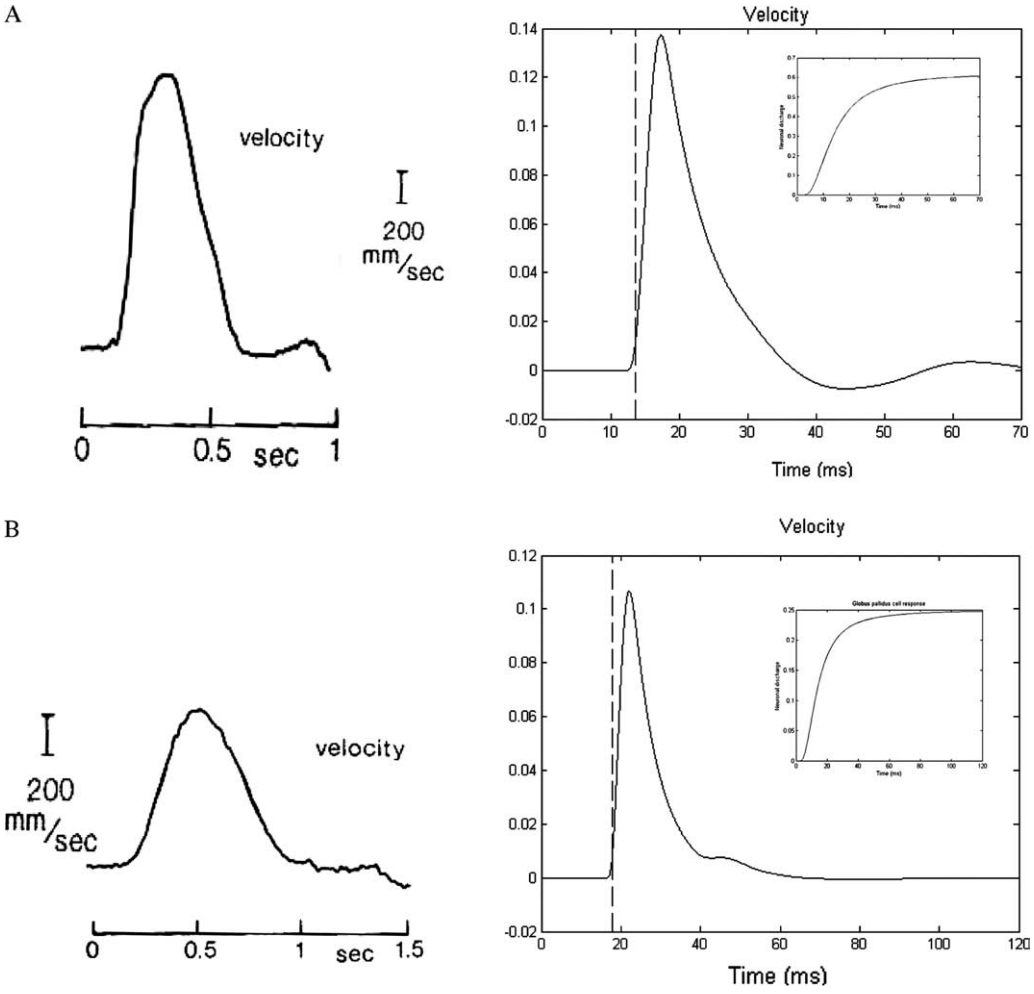

Fig. 12. Comparison of simulated (column 2) and experimentally obtained (column 1; reproduced with permission from Godaux et al., 1992, Fig. 3, p. 96, Copyright© Wiley-Liss, Inc., a subsidiary of John Wiley & Sons, Inc) velocity profile in normal (A) and PD (B) conditions. Insets: GO signal dynamics in normal (A) and PD (B) conditions. Parameter set (PD condition): $G_0=0.2$, $\beta=100.5$, $\gamma=0.8$, $DA_{1,3,4,8}=0.9$, $DA_{2,6,7}=0.8$, $DA_5=0.95$. Time units in ms.

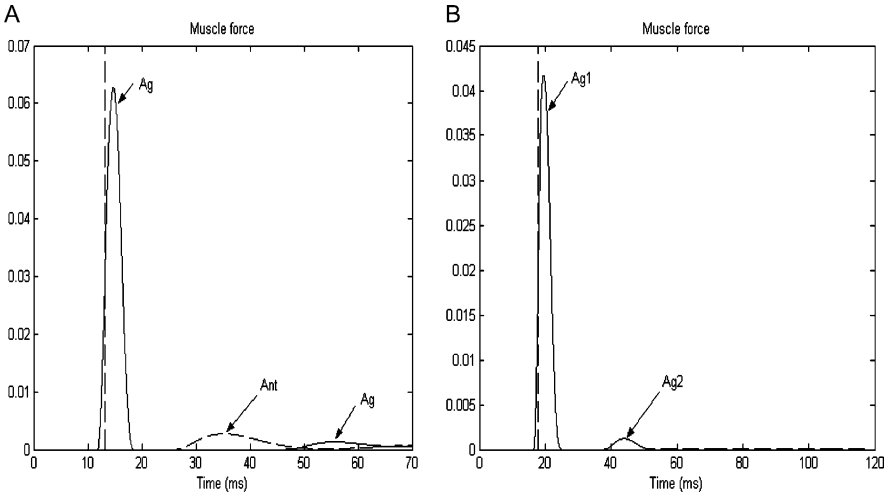

Fig. 13. Comparison of simulated normal (A) and PD (B) muscle force. Arrows indicate agonist–antagonist bursts. Parameter set (PD condition): $G_0=0.2$, $\beta=100.5$, $\gamma=0.8$, $DA_{1,3,4,8}=0.9$, $DA_{2,6,7}=0.8$, $DA_5=0.95$. Time units in ms.

et al., 1992) and simulated (column 2) velocity traces in normal (Fig. 12A) and PD (Fig. 12B) cases. The insets display the dynamics of the GO signals used. In normal case, the velocity profile was characterized by a single-peak and smooth velocity profile (Abend, Bizzi, & Morasso, 1982). As if the control subject smoothly accelerated until reaching maximum speed and then decelerated during the rest of the movement (Abend et al., 1982). In contrast, the velocity profile of the dopamine depleted case showed a reduced peak velocity and an increased time-to-peak time and movement duration (Camarata et al., 1992; Watts & Mandir, 1992; Weiss et al., 1996).

Fig. 13 shows model simulated muscle force curves in normal (Fig. 13A) and PD (Fig. 13B) cases, respectively. In the control (normal) case, a distinct agonist–antagonist–agonist pattern of muscle activation is observed (Fig. 13A). This pattern is disrupted when dopamine is depleted from the network. As it is reported experimentally (Stelmach, Teasdale, Phillips, & Worringham, 1989), the maximum peak force is reduced and the time-to-peak force is increased. In model simulations, the maximum peak force value was reduced from 0.062 to 0.04. A complete abolishment of the antagonist burst and an almost complete abolishment of the second agonist burst (its peak value is less than 0.001) is also observed (Fig. 12B; Berardelli et al., 1986).

Fig. 14 depicts multiple velocity curves as the output of BG and DA in the cortex and spinal cord are depleted. Clearly it can be seen that RT increases with increasingly larger amounts of DA depletion. Motor impairment is more apparent at 'medium' levels of DA depletion (dotted lines). Also, MT increases with decreasing levels of DA as seen from smaller peak velocities and longer velocity profiles (bradykinesia).

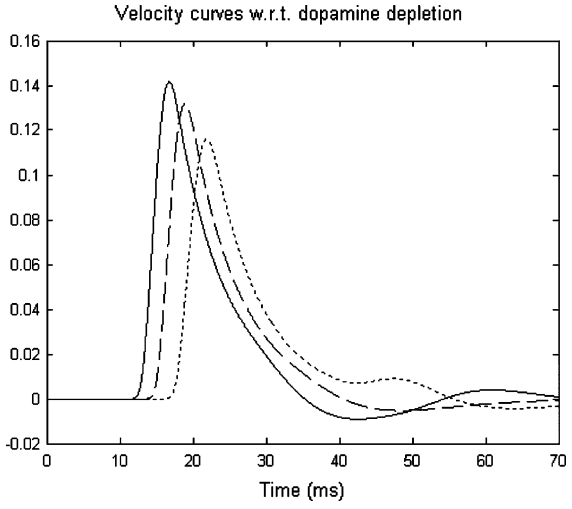

Fig. 14. Simulation of velocity curves when DA is progressively depleted in the model. Solid lines, normal ($G_0=0.6$, $\beta=100.5$, $\gamma=0.8$, $DA_{1-8}=1$); Dashed lines, 'low' DA depletion ($G_0=0.4$, $\beta=100.5$, $\gamma=0.8$, $DA_1=0.95$, $DA_2=0.75$, $DA_3=0.85$, $DA_4=0.85$, $DA_5=0.95$, $DA_6=0.85$, $DA_7=0.85$, $DA_8=0.95$); Dotted lines, 'medium' DA depletion ($G_0=0.2$, $\beta=100.5$, $\gamma=0.8$, $DA_1=0.9$, $DA_2=0.7$, $DA_3=0.8$, $DA_4=0.8$, $DA_5=0.9$, $DA_6=0.8$, $DA_7=0.8$, $DA_8=0.9$). 'Medium' and 'low' DA depletion simulation cases describe the parameter set values used to generate the corresponding velocity curves. Note that, as the amount of DA decreases, the output of the network shows increased reaction time, and slowness of movement (bradykinesia). Time units are in ms.

The model predicts that the degree of motor impairment is correlated with the amount of DA depletion.

Fig. 15 depicts the velocity (B), position (C) and muscle force (D) traces of large amplitude movements. As mentioned in the previous section, multiple motor programs in the form of a repetitive biphasic pattern of MN activation (Fig. 10) were needed to complete the movement. The termination of each motor program and the subsequent initiation of the next are clearly displayed by the inflection points on the PD position curve (Fig. 15C). The velocity (Fig. 15B) and muscle force (Fig. 15D) curves displayed multiple peaks and tended to show a prolonged deceleration phase (increased deceleration time; see Fig. 4 for schematic definition) as opposed to the normal case.

4.4. End-point movement variability

Camarata et al. (1992) recorded velocity and acceleration profiles for both pre- and post-MPTP cases, while monkeys were making two-joint horizontal planar movements to different directions. They reported a marked variability in the onset, peak velocity and time-course of the velocity profiles of MPTP-treated monkeys (Fig. 16A). In a similar study but with humans, Stelmach et al. (1989) reported variability in the force profile of PD patients.

Fig. 16 shows the comparison of the velocity profiles to a single target of a post-MPTP monkey (Fig. 16A) and the simulated velocity curves (Fig. 16B) of the dopamine-depleted model. As Fig. 16B depicts, our model was able to reproduce the variability in the onset, end, peak, time-course of the velocity profile as it is observed in kinematics studies (Camarata et al., 1992; Rand et al., 2000; Stelmach et al., 1989). To do so, we allowed the cortical, and spinal cord dopamine levels to take values from a uniform distribution bounded by 0.3 (lesioned) and 1 (normal). Using MATLAB's *unifrnd()* function, we generated six random values, which we used for DA values. In contrast, GO signal's G_0 and β were varied manually in order to produce smooth velocity profiles. For each of the DA random value, we let the model run, each time collecting the velocity and time vectors. At the end, we plotted all six velocity vectors with respect to time in one graph (Fig. 16B).

4.5. Which site has the 'strongest' effects on neuronal, EMG, and movement variables?

So far we have studied the effects of BG disrupted output and of dopamine depletion in cortex and spinal cord on the activity of neurons in the primary motor cortex, on EMG activity, and on movement variables such as reaction time and movement time. The question that arises is which disrupted site has the strongest effects on these variables? The output of the basal ganglia, or the cortex and the spinal cord? To answer this question, we identified three cases. In case 1, both cortical and spinal DA levels were depleted, whereas the output of the basal ganglia (GO signal) was unaltered (see Table 2, for DA_{1-8} parameter values in normal, 'low' and 'medium' simulated

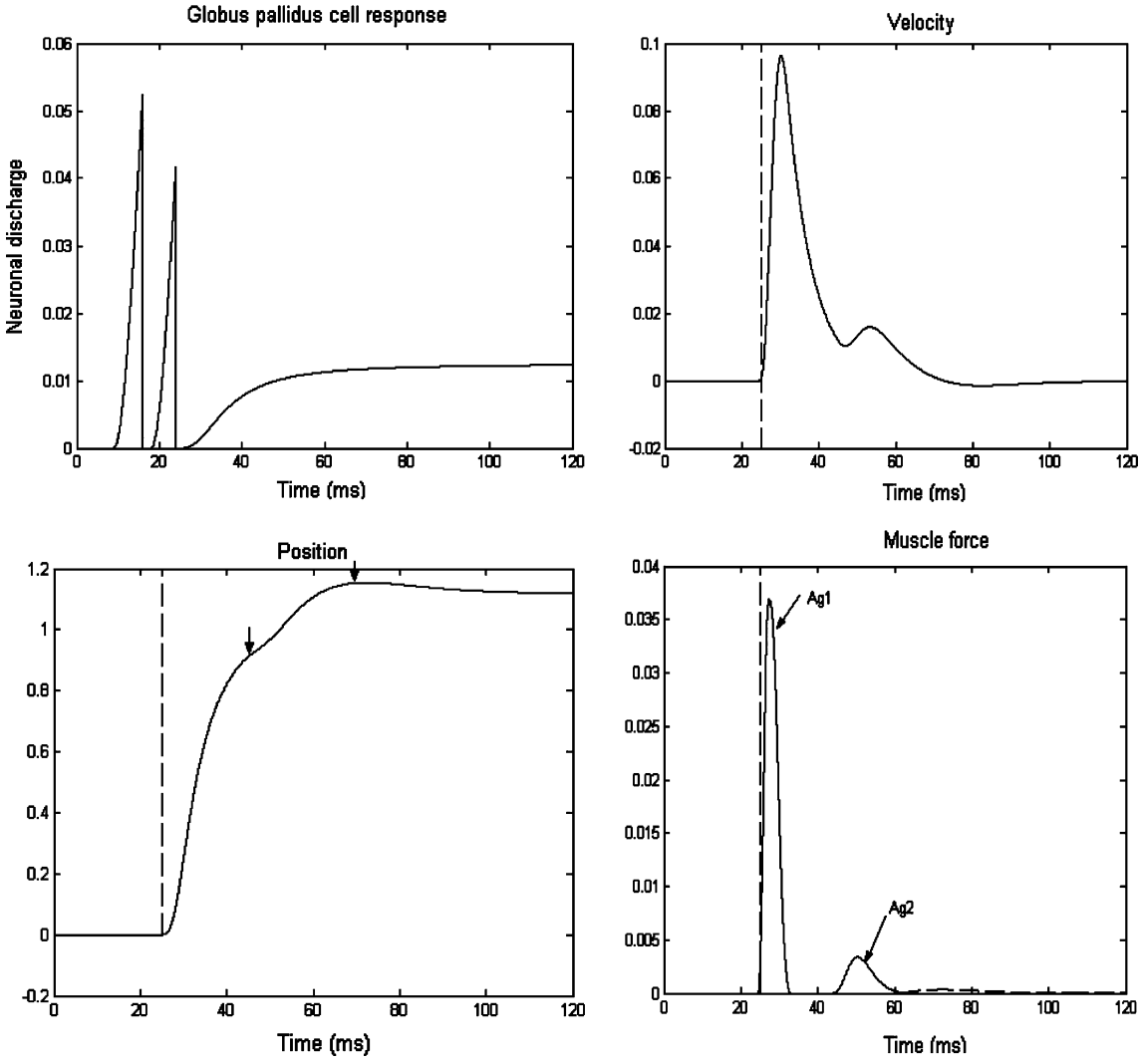

Fig. 15. Simulated GO signal (A), velocity (B), position (C) and muscle force (D) profiles in a large amplitude movement in dopamine-depleted condition. In A, repetitive GO signal dynamics is depicted. In *C*, down pointing arrows indicate sub-movements (inflection points) needed to complete the main movement. In D, two agonist bursts are needed to complete the movement, whereas antagonist bursts are abolished. Vertical dashed bar indicate the onset of movement (OM). Parameter set: $G_0=0.15$, $\beta=100.5$, $\gamma=0.8$, $DA_{1,3,4,8}=0.9$, $DA_{2,6,7}=0.8$, $DA_5=1$, all other parameters did not change. Time units are in ms.

conditions). In case 2, the output of the basal ganglia was reduced (see Table 2 for altered β and G_0 parameter values), where the cortical and spinal DA levels were held normal. In case 3, both the output of the basal ganglia and the DA cortical and spinal levels were depleted (see Table 2, for β, G_0, and DA_{1-8} parameter values). In all three cases, the effects of BG disrupted output and of cortical and spinal DA depletion on neuronal, muscular, and movement variables were studied for three conditions: (1) normal (no disruption), (2) 'low' disruption, and (3) 'medium' disruption.

In case 1, cortical and spinal DA levels were progressively depleted. The DA parameter values and the results in all three simulated conditions (see above) are summarized in Table 2. The effects of the cortical and spinal DA depletion are clearly seen on peak DVV activity (0.21 at 0%, 0.20 at 10%, and 0.19 at 25% DA depletion), peak EMG activity (1.59 at 0%, 1.4 at 10% and 1.28 at 25%), reaction time (4.39 ms at 0%, 4.94 ms at 10%, 5.45 ms at 25%), movement time (14.77 ms at 0%, 16.89 ms at 10% and 17.16 ms at 25%) and time-to-peak velocity (2.99 ms at 0%, 3.36 ms at 10%, 3.65 ms at 25%). Inconsistent results were produced for the peak velocity (V_{max}), deceleration time (DT), and muscle force (F). More specifically, V_{max} dropped from 0.11 at 0% DA depletion to 0.09 at 10% DA depletion. No change in peak velocity was observed at lower percentages of DA depletion. Similarly, DT was increased from 11.79 at 0% to 13.53 at 10% and remained there at 25% DA depletion, whereas F was lowered to 0.04 at 10% and remained constant to that value at 25%.

In case 2, the effects of the depleted BG output in the form of a reduced in size and rate of change GO signal (see case 2 of Table 2 for values of β and G_0 parameters) on neuronal, muscular, and movement variables, were studied. The reduced size and rate of the GO signal alludes to the unresponsive nature of the GPi cells in MPTP primates (Chevalier & Deniau, 1990; Filion, Tremblay, & Bedard, 1991; Tremblay et al., 1989). The dopamine levels in the cortex and spinal cord remained unaltered ($DA_{1-8}=1$). The effects of BG DA depletion gave more consistent results (see Table 2 for

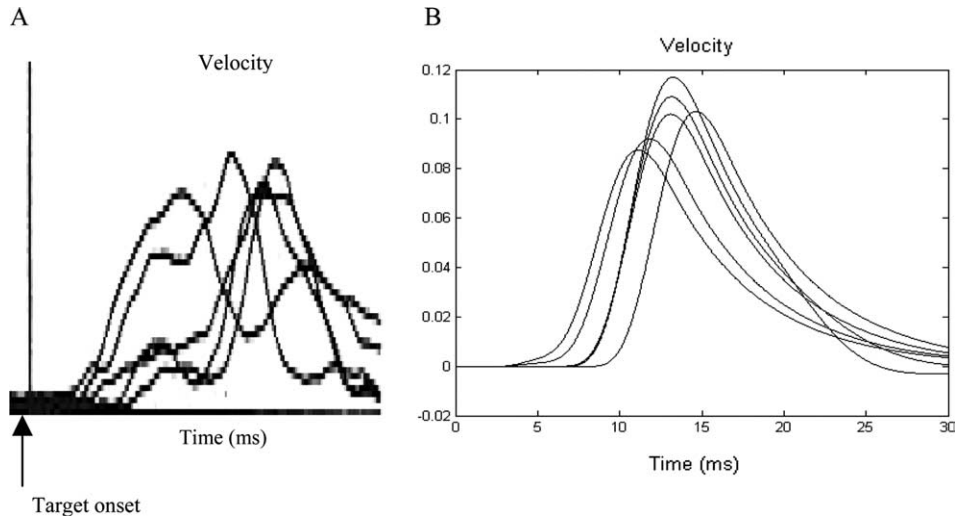

Fig. 16. Comparison of velocity profiles to a single target for post-MPTP (A) (reproduced with permission from Camarata et al., 1992, Fig. 4, p. 612, Copyright© Elsevier Science Ltd) and simulated dopamine-depleted (B) conditions. In A, profiles are aligned on target presentation (vertical bar). Note the variability in the onset, end, peak velocity and time course of the velocity profiles in both experimentally MPTP-treated and simulated DA depleted conditions.

neuronal, EMG, and movement variable values). MT, RT, TPV, and DT increased, whereas peak DVV, peak EMG, muscle force activities and peak velocity were reduced, as we go from the normal condition to the 'medium' disrupted condition. The profile of the GO signal used in these simulations had a sigmoidal shape (see inset of Fig. 12B).

In case 3, both the output of BG and the cortical and spinal DA levels were reduced. The results followed the same pattern as in case 2, but the effects in this case were more severe (see case 3 of Table 2 for parameter and neuronal, EMG, and movement variable values).

5. Discussion

5.1. General issues

The present model is a model of voluntary movement and proprioception that offers an integrated interpretation of the functional roles of the diverse cell types in movement related areas of the primate cortex. The model is an extension and revision of the VITE-FLETE model of Contreras-Vidal et al. (1997), which addressed primarily psychophysical data and provided neural interpretations for the variables DV, DVV, PPV, and GO. The model is based on known cortico-spinal neuroanatomical connectivity (see Tables 1 and 2 of Contreras-Vidal et al., 1997). Its dynamic activity matched that of the neural firing pattern of dominant cell types in primary motor cortex (area 4) and parietal cortex (area 5), such as reciprocal neurons, bidirectional neurons, phasic MT neurons, tonic neurons, etc., known to be necessary for voluntary normal and parkinsonian (bradykinesia) reaching tasks.

The model provides an integrative perspective on cortico-spinal control of parkinsonian voluntary movement by studying the effects of dopamine depletion on the output of the basal ganglia, cortex and spinal cord. It accounts of many known empirical signatures of Parkinsonian willful action such as

- Increased cellular reaction time
- Prolonged behavior reaction time
- Increased duration of neuronal discharge in area 4 preceding and following onset of movement
- Reduction of firing intensity and firing rate of cells in primary motor cortex
- Abnormal oscillatory GPi response
- Disinhibition of reciprocally tuned cells
- Increases in baseline activity
- Repetitive bursts of muscle activation
- Prolongation of premotor and electromechanical delay times
- Reduction in the size and rate of development of the first agonist burst of EMG activity
- Asymmetric increase in the time-to-peak and deceleration time
- Decrease in the peak value of the velocity trace
- ncrease in movement duration
- Substantial reduction in the size and rate of development of muscle production
- Movement variability.

These findings provide enough evidence to support the main hypothesis of the model reported earlier in the paper (see last paragraph of introduction).

5.2. What do we learn from the model?

One of the new predictions the model makes is first of all the functional role for the activity of bidirectional neurons found in primary motor cortex (Doudet et al., 1990) in the form of a central co-contraction signal sent to the antagonist muscles during the generation of voluntary movement. Humphrey & Reed (1983) were the first to report on the presence of such

Table 2
Effects of disrupted BG output and dopamine depletion on neuronal, muscular and movement variables in three cases

	Normal	'Low' disruption	'Medium' disruption
Case 1	Normal BG output, but DA depleted cortical and spinal sites		
G_0	0.6	0.6	0.6
β	15.5	15.5	15.5
Γ	1	1	1
$DA_{1,3,4,7}$	1	0.9	0.75
$DA_{2,6,8}$	1	0.8	0.65
DA_5	1	1	1
DVV_{max}	0.21	0.20	0.19
EMG_{max}	1.59	1.4	1.28
V_{max}	0.11	0.09	0.09
RT (ms)	4.39	4.94	5.45
TPV (ms)	2.99	3.36	3.65
DT (ms)	11.79	13.53	13.51
MT (ms)	14.77	16.89	17.16
F	0.06	0.04	0.04
Case 2	Normal DA cortical and spinal sites, but disrupted BG output		
G_0	0.6	0.54	0.45
β	15.5	16.55	19.4
Γ	1	1	1
$DA_{1,3,4,7}$	1	1	1
$DA_{2,6,8}$	1	1	1
DA_5	1	1	1
DVV_{max}	0.21	0.20	0.18
EMG_{max}	1.59	1.54	1.43
V_{max}	0.11	0.096	0.0751
RT (ms)	4.39	4.55	4.94
TPV (ms)	2.99	3.23	3.95
DT (ms)	11.79	13.63	13.80
MT (ms)	14.77	16.86	17.75
F	0.06	0.051	0.0325
Case 3	Disrupted BG output and DA depleted cortical and spinal sites		
G_0	0.6	0.54	0.45
β	15.5	16.55	19.4
Γ	1	1	1
$DA_{1,3,4,7}$	1	0.9	0.75
$DA_{2,6,8}$	1	0.8	0.65
DA_5	1	1	1
DVV_{max}	0.21	0.19	0.17
EMG_{max}	1.59	1.35	1.15
V_{max}	0.11	0.08	0.08
RT (ms)	4.39	5.15	6.71
TPV (ms)	2.99	3.72	4.42
DT (ms)	11.79	13.55	13.41
MT (ms)	14.77	17.27	17.83
F	0.06	0.04	0.03

Note that 'Low' and 'Medium' disruption conditions reflect the changes in the BG output and/or in cortical and spinal DA parameter values in each case.

a signal. Their pioneering work was the first direct neurophysiological evidence for the existence of two separate central systems: one organized for reciprocal activation of antagonist muscles, and another for their coactivation. Humphrey & Reed (1983) failed to provide the pathway from which their coactivation cells exert their influence onto the flexor and extensor MNs. Other modeling work (Bullock & Contreras-Vidal, 1993) envisioned the co-contractive signal to be a tonically active signal that is present throughout the movement. In our model, the influence of the coactivation cells on the flexor and extensor MNs is controlled by the activities of the bidirectional neurons (Eq. (4)), which is represented by the gating of the DV input by a voluntarily scalable GO signal to primary motor cortex.

With this model, we predicted that the origin of the repetitive triphasic pattern of muscle activation observed in Parkinson's disease movements is a central one. It originates from the oscillatory output of the basal ganglia structures, specifically of the globus pallidus internal segment (Tremblay et al., 1989). Tremblay and colleagues (1989) showed that MPTP-treated GPi produces oscillatory responses, which comprise of at least two inhibition-excitation sequences (see Fig. 8A). Hallett & Khoshbin (1980) demonstrated that for fast, but accurate elbow flexion movements, PD patients required additional triphasic patterns of muscle activation in order to complete the movements. Each cycle required a fixed amount of time, but the magnitudes of their bursts were smaller in each subsequent cycle. In order for our model to produce such an oscillatory behavior, the pallidal output tonic activation (i.e. GO signal) had to be initiated and interrupted many times in a single movement (see Fig. 15A). Each GO signal activation cycle had a fixed amount of time, but its magnitude was smaller in each subsequent cycle. Each cycle represented the motor command sent to the lower spinal centers, so that the appropriate muscle recruitment level was generated to complete the movement. Since each activation cycle did not generate the appropriate level of muscle activation, so that the movement could be completed with a single set of agonist–antagonist bursts, additional biphasic bursts of lower intensities were needed to complete the movement (see Figs. 10 and 15B–D).

Moreover, our model simulates successfully the variability in the onset, end, peak, and time-course of the velocity profiles (movement variability) observed in Parkinson's disease kinematics studies (Camarata et al., 1992; Rand et al., 2000; Stelmach et al., 1989). In the model, the parameters of the GO signal (BG output) and the dopamine levels in cortex and spinal cord were allowed to vary randomly from trial to trial. We believe that such an assumption for a random variability in BG output and in cortical and spinal DA levels maybe a reasonable one, since it has long been recognized that the random firing mode is the predominating firing mode of DAergic neurons in the rat (Bunney et al., 1973; Grace & Bunney, 1984a,b; Tepper, Martin, & Anderson, 1995). Furthermore, it has been found that damage to the nigrostriatal pathway following PD, causes a profound reduction of DA content in the SNc (more 90% of DA neurons die (Burns, Chiueh, Markey, Ebert, Jacobowitz and Kopin, 1983)). That means that the remaining DA neurons have to compensate for that loss and therefore undergo a transformation, where they modify their firing patterns (Bezard & Gross, 1998; Grace, 1995). So, for example when the firing rate of DA neurons is low, they might not facilitate adequately the motor cortical commands send to the lower spinal centers and hence the subject's arm might not be able to reach the target (undershoot). In the next trial, the DA neurons might increase their firing rates to compensate for the subject's

behavioral dysfunction, and hence over-facilitated motor cortical command would cause the subject's arm to either reach the target or overshoot the target. This is of course a thought experiment that needs to be investigated more thoroughly by neurophysiologists.

Finally, our model provides an extensive analysis on which site has the strongest effect on neuronal, EMG and movement variables when its dopamine levels are dropped. Our analysis suggests that while the disrupted basal ganglia output has the strongest effect on movement, dopamine depletion in the cortex and spinal cord is needed to strengthen and refine these results. We believe that this is a reasonable assumption, because the dopamine levels in the cortex are only 5–10%, whereas in the basal ganglia are 90–95% (Tzschentke, 2001).

5.3. Model limitations and failures

Although our model is successful in simulating many aspects of PD bradykinesia, it has also few shortcomings. First, the model does not account for learning of movements, since it assumes that the movement is already learned and stored in motor areas. Second, it does not account for a detailed circuit of the basal ganglia structures. In the model, the effect of the basal ganglia structures comes in the form of GO signal that is multiplied with area 4 cell activity to generate volitional command that is sent to spinal centers for the generation of movement. Third, it does not account for the effects of dopamine depletion on the long-latency stretch response. There is evidence that the gain of long-latency stretch responses is abnormally high in-patients with PD (Rothwell, Obeso, Traub, & Marsden, 1983). These responses are elicited by muscle stretch and occur later than the segmental stretch reflex. The circuitry underlying the long-latency responses has been subject of intense debate. Some researchers (Mathews, 1972) suggest that afferent signals reach the cortex to activate corticospinal neurons, whereas others (Hagbarth, Hagglund, Wallin, & Young, 1981) believe that reflexes are spinal with the long-latency attributable to delayed afferent input. Fourth, although in the model, there are spinal inhibitory interneurons, the model does not take into account the effects of dopamine depletion on their activities. Delwaide and colleagues (1991) have suggested that rigidity observed in PD patients is due to increased excitability of motor neurons because of reduced activity of spinal inhibitory interneurons.

5.4. Future extensions

Work is underway in our laboratory to address some of the shortcomings of the model presented earlier. A more detailed BG model based on works by Brown et al. (2004) and Contreras-Vidal (1999) as well as on other BG models (Gurney, Prescott, & Redgrave, 2001a,b; Taylor & Taylor, 2000) that will account for all the known detailed anatomical, neurochemical and neurophysiological evidence of basal ganglia structures, will be added to the current detailed cortico-spinal network. Also, the effects of dopamine depletion on spinal inhibitory interneurons and how their activity affects spinal reflexes will be studied more carefully. These findings will extend the present model to other PD symptoms such as rigidity, akinesia and tremor. We believe that all of these improvements will produce a more comprehensive and detailed neural model of basal ganglia-thalamo-cortico-spinal interactions, and hence we will be able to study more systematically the effects of dopamine depletion and integrate into a 'unified theory' all the known neurophysiological, EMG and behavioral observations of Parkinson's disease.

Acknowledgements

First author would like to thank Prof. Daniel Bullock for thoughtful conversations during the embryonic stage of this research.

References

Abbs, J. H., Hartman, D. E., & Vishwanat, B. (1987). Orofacial motor control impairment in Parkinson's disease. *Neurology*, *37*, 394–398.

Abend, W., Bizzi, E., & Morasso, P. (1982). Human arm trajectory formation. *Brain*, *105*(Pt. 2), 331–348.

Albin, R. L., Young, A. B., & Penney, J. B. (1989). The functional anatomy of basal ganglia disorders. *Trends in Neurosciences*, *12*, 366–375.

Bathien, N., & Rondot, P. (1977). Reciprocal continuous inhibition in rigidity in parkinsonism. *Journal of Neurology, Neurosurgery, and Psychiatry*, *40*, 20–24.

Benazzouz, A., Gross, C., Dupont, J., & Bioulac, B. (1992). MPTP induced hemiparkinsonism in monkeys: Behavioral, mechanographic, electromyographic and immunohistochemical studies. *Experimental Brain Research*, *90*, 116–120.

Benecke, R., Rothwell, J. C., & Dick, J. P. R. (1986). Performance of simultaneous movements in patients with Parkinson's disease. *Brain*, *109*, 739–757.

Berardelli, A., Dick, J. P. R., Rothwell, J. C., Day, B. L., & Marsden, C. D. (1986). Scaling of the size of the first agonist EMG burst during rapid wrist movements in patients with Parkinson's disease. *Journal of Neurology, Neurosurgery, and Psychiatry*, *49*, 1273–1279.

Berger, B., Trottier, S., Verney, C., Gaspar, P., & Alvarez, C. (1988a). Regional and laminar distribution of dopamine and serotonin innervation in the macaque cerebral cortex: A radioautographic study. *The Journal of Comparative Neurology*, *273*, 99–119.

Berns, G., & Sejnowski, T. (1998b). A computational model of how the basal ganglia produce sequences. *Journal of Cognitive Neuroscience*, *10*, 108–121.

Bezard, E., & Gross, C. E. (1998c). Compensatory mechanisms in experimental and human parkinsonism: Towards a dynamic approach. *Progress in Neurobiology*, *55*, 93–116.

Bjorklund, A., & Lindvall, O. (1984). Dopamine containing systems in the CNS. In A. Bjorklund, & T. Hokfelt (Vol. Eds), *Handbook of chemical neuroanatomy. Classical transmitters in the CNS, Part 1* (Vol. 2) (pp. 55–121). Amsterdam: Elsevier.

Bjorklund, A., & Skagerberg, G. (1979). Evidence of a major spinal cord projection from the diencephalic A11 dopamine cell group in the rat using transmitter-specific fluoroscent retrograde tracing. *Brain Research*, *177*, 170–175.

Blessing, W. W., & Chalmers, J. P. (1979). Direct projection of catecholamine (presumably dopamine)-containing neurons from the hypothalamus to spinal cord. *Neuroscience Letters*, *11*, 35–40.

Brown, S. H., & Cooke, J. D. (1984). Initial agonist burst duration depends on movement amplitude. *Experimental Brain Research*, *55*, 523–527.

Brown, S. H., & Cooke, J. D. (1990a). Movement related phasic muscle activation I. Relations with temporal profile of movement. *Journal of Neurophysiology*, *63*(3), 455–464.

Brown, S. H., & Cooke, J. D. (1990b). Movement related phasic muscle activation II. Generation and functional role of the triphasic pattern. *Journal of Neurophysiology*, *63*(3), 465–472.

Brown, J. W., Bullock, D., & Grossberg, S. (2004). How laminar frontal cortex and basal ganglia circuits interact to control planned and reactive saccades. *Neural Networks*, *17*, 471–510.

Bullock, D., Cisek, P., & Grossberg, S. (1998). Cortical networks for control of voluntary arm movements under variable force conditions. *Cerebral Cortex*, *8*, 48–62.

Bullock, D., & Contreras-Vidal, J. L. (1993). How spinal neural networks reduce discrepancies between motor intention and motor realization. In K. Newel, & D. Corcos (Eds.), *Variability and motor control* (pp. 183–221). Champaign, IL: Human Kinetics Press.

Bullock, D., & Grossberg, S. (1988). Neural dynamics of planned arm movements: Emergent invariants and speed-accuracy properties during trajectory formation. *Psychological Review*, *95*, 49–90.

Bullock, D., & Grossberg, S. (1989). VITE and FLETE: Neural modules for trajectory formation and tension control. In W. Hershberger (Ed.), *Volitional action* (pp. 253–297). Amsterdam, The Netherlands: North-Holland.

Bullock, D., & Grossberg, S. (1991). Adaptive neural networks for control of movement trajectories invariant under speed and force rescaling. *Human Movement Science*, *10*, 3–53.

Bullock, D., & Grossberg, S. (1992). Emergence of triphasic muscle activation from the nonlinear interactions of central and spinal neural networks circuits. *Human Movement Science*, *11*, 157–167.

Bunney, B. S., Walters, J. R., Roth, R. H., & Aghajanian, G. K. (1973). Dopaminergic neurons: Effect of antipsychotic drugs and amphetamine on single cell activity. *The Journal of Pharmacology and Experimental Therapeutics*, *185*, 560–571.

Burns, R. S., Chiueh, C. C., Markey, S. P., Ebert, M. N., Jacobowitz, D. M., & Kopin, I. J. (1983). A primate model of parkinsonism: Selective destruction of dopaminergic neurons in the pars compacta of the substantia nigra by *N*-methyl-4-phenyl-1,2,3,6-tetrahydropyridine. *Proceedings of the National Academy of Sciences USA*, *80*, 4546–4550.

Camarata, P. J., Parker, R. G., Park, S. K., Haines, S. J., Turner, D. A., Chae, H., et al. (1992). Effects of MPTP induced hemiparkinsonism on the kinematics of a two-dimensional, multi-joint arm movement in the rhesus monkey. *Neuroscience*, *48*(3), 607–619.

Chapman, C. D., Spidalieri, G., & Lamarre, Y. (1984). Discharge properties of area 5 neurons during arm movements triggered by sensory stimuli in the monkey. *Brain Research*, *309*, 63–77.

Chevalier, G., & Deniau, M. J. (1990). Disinhibition as a basic process in the expression of striatal functions. *Trends in Neuroscience*, *13*(7), 277–280.

Commissiong, J. W., Gentleman, S., & Neff, N. H. (1979). Spinal cord dopaminergic neurons: Evidence for an uncrossed nigrostriatal pathway. *Neuropharmacology*, *18*, 565–568.

Connor, N. P., & Abbs, J. H. (1991). Task-dependent variations in parkinsonian motor impairments. *Brain*, *114*, 321–332.

Contreras-Vidal, J. L. (1999). The gating functions of the basal ganglia in movement control. In J. A. Reggia, E. Ruppin, & D. Glanzman (Vol. Eds.), *Progress in brain research* (Vol. 121).

Contreras-Vidal, J. L., Grossberg, S., & Bullock, D. (1997). A neural model of cerebellar learning for arm movement control: Cortico-spino-cerebellar dynamics. *Learning and Memory*, *3*(6), 475–502.

Contreras-Vidal, J. L., & Stelmach, G. (1995). A neural model of basal ganglia-thalamocortical relations in normal and parkinsonian movement. *Biological Cybernetics*, *73*, 467–476.

Corcos, D. M., Chen, C. M., Quinn, N. P., McAuley, J., & Rothwell, J. C. (1996). Strength in Parkinson's disease: Relationship to rate of force generation and clinical status. *Annals of Neurology*, *39*(1), 79–88.

Delwaide, P. J., Pepin, J. L., & Maertens de Noordhout, A. (1991). Short-latency autogenic inhibition in patients with parkinsonian rigidity. *Annals of Neurology*, *30*, 83–89.

Dormand, J. R., & Prince, P. J. (1980). A family of embedded Runge-Kutta formulae. *Journal of Computational and Applied Mathematics*, *6*, 19–26.

Doudet, D. J., Gross, C., Arluison, M., & Bioulac, B. (1990). Modifications of precentral cortex discharge and EMG activity in monkeys with MPTP induced lesions of DA nigral lesions. *Experimental Brain Research*, *80*, 177–188.

Doudet, D. J., Gross, C., Lebrun-Grandie, P., & Bioulac, B. (1985). MPTP primate model of Parkinson's disease: A mechanographic and electromyographic study. *Brain Research*, *335*, 194–199.

Dubois, A., Savasta, M., Curet, O., & Scatton, B. (1986). Autoradiographic distribution of the D_1 agonist [^{3}H]SKF 38393, in the rat brain and spinal cord. Comparison with the distribution of D_2 dopamine receptors. *Neuroscience*, *19*, 125–137.

Elsworth, J. D., Deutch, A. Y., Redmond, D. E., Sladek, J. R., & Roth, R. H. (1990). MPTP reduces dopamine and norepinephrine concentrations in the supplementary motor area and cingulate cortex of the primate. *Neuroscience Letters*, *114*, 316–322.

Filion, M., Tremblay, L., & Bedard, P. J. (1991). Effects of dopamine agonists on the spontaneous activity of globus pallidus neurons in monkeys with MPTP-induced parkinsonism. *Brain Research*, *547*(1), 152–161.

Flowers, K. A. (1976). Visual 'closed-loop' and 'open-loop' characteristics of voluntary movement in patients with Parkinsonism and intention tremor. *Brain*, *99*(2), 269–310.

Fromm, C., Wise, S. P., & Evarts, E. V. (1984). Sensory response properties of pyramidal tract neurons in the precentral motor cortex and postcentral gyrus of the rhesus monkey. *Experimental Brain Research*, *54*, 177–185.

Gaspar, P., Duyckaerts, C., Alvarez, C., Javoy-Agid, F., & Berger, B. (1991). Alterations of dopaminergic and noradrenergic innervations in motor cortex in Parkinson's disease. *Annals of Neurology*, *30*, 365–374.

Gaspar, P., Stepniewska, I., & Kaas, J. H. (1992). Topography and collateralization of the dopaminergic projections to motor and lateral prefrontal cortex in owl monkeys. *The Journal of Comparative Neurology*, *325*, 1–21.

Georgopoulos, A. P., Kalaska, J. F., Caminiti, R., & Massey, J. T. (1982). On the relations between the direction of two dimensional arm movements and cell discharge in primate motor cortex. *The Journal of Neuroscience*, *2*, 1527–1537.

Ghez, C., & Gordon, J. (1987a). Trajectory control in targeted force impulses. I. Role in opposing muscles. *Experimental Brain Research*, *67*, 225–240.

Ghez, C., & Gordon, J. (1987b). Trajectory control in targeted force impulses. II. Pulse height control. *Experimental Brain Research*, *67*, 241–252.

Ghez, C., & Gordon, J. (1987c). Trajectory control in targeted force impulses. III. Compensatory adjustments for initial errors. *Experimental Brain Research*, *67*, 253–269.

Gibberd, F. B. (1986). The management of Parkinson's disease. *The Practitioner*, *230*, 139–146.

Godaux, E., Koulischer, D., & Jacquy, J. (1992). Parkinsonian bradykinesia is due to depression in the rate of rise of muscle activity. *Annals of Neurology*, *31*(1), 93–100.

Gottlieb, G. L., Latash, M. L., Corcos, D. M., Liubinskas, A. J., & Agarwal, G. C. (1992). Organizing principle for single joint movements: I. Agonist–antagonist interactions. *Journal of Neurophysiology*, *13*(6), 1417–1427.

Grace, A. A. (1995). The tonic/phasic model of dopamine system regulation: Its relevance for understanding how stimulant abuse can alter basal ganglia function. *Drug and Alcohol Dependence*, *37*, 111–129.

Grace, A. A., & Bunney, B. S. (1984a). The control of firing pattern in nigral dopamine neurons: Burst firing. *The Journal of Neuroscience*, *4*, 2877–2890.

Grace, A. A., & Bunney, B. S. (1984b). The control of firing pattern in nigral dopamine neurons: Single spike firing. *The Journal of Neuroscience*, *4*, 2866–2876.

Gross, C., Feger, J., Seal, J., Haramburu, P., & Bioulac, B. (1983). Neuronal activity of area 4 and movement parameters recorded in trained monkeys after unilateral lesion of the substantia nigra. *Experimental Brain Research*, *7*, 181–193.

Gurney, K., Prescott, T. J., & Redgrave, P. (2001a). A computational model of action selection in the basal ganglia. I. A new functional anatomy. *Biological Cybernetics*, *84*, 401–410.

Gurney, K., Prescott, T. J., & Redgrave, P. (2001b). A computational model of action selection in the basal ganglia. II. Analysis and simulation of behavior. *Biological Cybernetics*, *84*, 411–423.

Hagbarth, K. E., Hagglund, J. V., Wallin, E. U., & Young, R. R. (1981). Grouped spindle and electromyographic responses to abrupt wrist extension movements in man. *Journal of Physiology (London)*, *312*, 81–96.

Hagbarth, K. E., Wallin, G., Lofstedt, L., & Aquilonius, S. M. (1975). Muscle spindle activity in alternating tremor of Parkinsonism and in clonus. *Journal of Neurology, Neurosurgery, and Psychiatry*, *38*(7), 636–641.

Hallett, M., & Khoshbin, S. (1980). A physiological mechanism of bradykinesia. *Brain*, *103*, 301–314.

Hallett, M., & Marsden, C. D. (1979). Ballistic flexion movements of the human thumb. *The Journal of Physiology*, *294*, 33–50.

Hayashi, A., Kagamihara, Y., Nakajima, Y., Narabayashi, H., Okuma, Y., & Tanaka, R. (1988). Disorder in reciprocal innervation upon initiation of voluntary movement in patients with Parkinson's disease. *Experimental Brain Research*, *70*, 437–440.

Henneman, E. (1957). Relation between size of neurons and their susceptibility to discharge. *Science*, *126*, 1345–1347.

Henneman, E. (1985). The size principle: A deterministic output emerges from a set of probabilistic connections. *The Journal of Experimental Biology*, *115*, 105–112.

Horak, F. B., & Anderson, M. E. (1984). Influence of globus pallidus on arm movements in monkeys. I. Effects of kainic acid-induced lesions. *Journal of Neurophysiology*, *52*, 290–304.

Humphrey, D. R., & Reed, D. J. (1983). Separate cortical systems for control of joint movement and joint stiffness: Reciprocal activation and coactivation of antagonist muscles. In J. E. Desmedt (Ed.), *Motor control mechanisms in health and disease*. New York: Raven Press.

Jankovic, J. (1987). Pathophysiology and clinical assessment of motor symptoms in Parkinson's disease. In W. C. Koller (Ed.), *Handbook of Parkinson's disease*.

Kalaska, J. F., Cohen, D. A. D., Hyde, M. L., & Prud'Homme, M. J. (1989). A comparison of movement direction-related versus load direction-related activity in primate motor cortex, using a two-dimensional reaching task. *The Journal of Neuroscience*, *9*, 2080–2102.

Kalaska, J. F., Cohen, D. A. D., Prud'Homme, M. J., & Hyde, M. L. (1990). Parietal area 5 neuronal activity encodes movement kinematics, not movement dynamics. *Experimental Brain Research*, *80*, 351–364.

Lazarus, J. C., & Stelmach, G. E. (1992). Inter-limb coordination in Parkinson's disease. *Movement Disorders*, *7*, 159–170.

Lewis, D. A., Morrison, J. H., & Goldstein, M. (1988). Brainstem dopaminergic neurons project to monkey parietal cortex. *Neuroscience Letters*, *86*, 11–16.

Lidow, M. S., Goldman-Rakic, P. S., Gallager, D. W., Geschwind, D. H., & Rakic, P. (1989). Distribution of major neurotransmitter receptors in the motor and somatosensory cortex of the rhesus monkey. *Neuroscience*, *32*(3), 609–627.

Mathews, P. B. C. (1972). *Mammalian muscle receptors and their central actions*. Baltimore, MD: Williams and Wilkins.

McCrea, D. A. (1992). Can sense be made of spinal interneurons circuits? *The Behavioral and Brain Sciences*, *15*, 635–829.

Obeso, J. A., Quesada, P., Artieda, J., & Martinez-Lage, J. M. (1985). Reciprocal inhibition in rigidity and dystonia. In P. J. Delwaide, & A. Agnoli (Eds.), *Clinical neurophysiology in Parkinsonism*. Amsterdam, The Netherlands: Elsevier Science Publishers BV.

Rand, M. K., Stelmach, G. E., & Bloedel, J. R. (2000). Movement accuracy constraints in Parkinson's disease patients. *Neuropsychologia*, *38*, 203–212.

Rothwell, J. C., Obeso, J. A., Traub, M. M., & Marsden, C. D. (1983). The behavior long-latency stretch reflex in patients with Parkinson's disease. *Journal of Neurology, Neurosurgery, and Psychiatry*, *46*, 35–44.

Scatton, B., Javoy-Agid, F., Rouquier, L., Dubois, B., & Agid, Y. (1983). Reduction of cortical dopamine, noradrenaline, serotonin and their metabolites in Parkinson's disease. *Brain Research*, *275*, 321–328.

Shirouzou, M., Anraku, T., Iwashita, Y., & Yoshida, M. (1990). A new dopaminergic terminal plexus in the ventral horn of the rat spinal cord. Immunohistochemical studies at the light and the electron microscopic levels. *Experientia*, *46*, 201–204.

Stelmach, G. E., Teasdale, N., Phillips, J., & Worringham, C. J. (1989). Force production characteristics in Parkinson's disease. *Experimental Brain Research*, *76*, 165–172.

Takada, M., Li, Z. K., & Hattori, T. (1988). Single thalamic dopaminergic neurons project to both neocortex and spinal cord. *Brain Research*, *455*, 346–352.

Taylor, J. G., & Taylor, N. R. (2000). Analysis of recurrent cortico-basal ganglia-thalamic loops for working memory. *Biological Cybernetics*, *82*, 415–432.

Teasdale, N., Philips, J., & Stelmach, G. E. (1993). Determining movement onsets from temporal series. *Journal of Motor Behavior*, *25*, 97–106.

Tepper, J. M., Martin, L. P., & Anderson, D. R. (1995). GABAA receptor mediated inhibition of rat substantia nigra dopaminergic neurons by pars reticulata projection neurons. *The Journal of Neuroscience*, *15*, 3092–3103.

Tremblay, L., Filion, M., & Bedard, P. J. (1989). Responses of pallidal neurons to striatal stimulation in monkeys with MPTP-induced parkinsonism. *Brain Research*, *498*(1), 17–33.

Tzschentke, T. M. (2001). Pharmacology and behavioral pharmacology of the mesocortical dopamine system. *Progress in Neurobiology*, *63*, 241–320.

Watts, R. L., & Mandir, A. S. (1992). The role of motor cortex in the pathophysiology of voluntary movement deficits associated with parkinsonism. *Neurologic Clinics*, *10*(2), 451–469.

Weil-Fugazza, J., & Godefroy, F. (1993). Dorsal and ventral dopaminergic innervation of the spinal cord: Functional implications. *Brain Research Bulletin*, *30*, 319–324.

Weiner, W. J., & Singer, C. (1989). Parkinson's disease and non-pharmacologic treatment programs. *Journal of the American Geriatrics Society*, *37*, 359–363.

Weiss, P., Stelmach, G. E., Adler, C. H., & Waterman, C. (1996). Parkinsonian arm movements as altered by task difficulty. *Parkinsonism and Related Disorders*, *2*(4), 215–223.

Wierzbicka, M. M., Wiegner, A. W., & Shahani, B. T. (1986). Role of agonist and antagonist muscles in fast arm movements in man. *Experimental Brain Research*, *63*, 331–340.

Williams, S. M., & Goldman-Rakic, P. S. (1995). Characterization of the dopaminergic innervation of the primate frontal cortex using a dopamine-specific antibody. *Cerebral Cortex*, *3*, 199–222.

Williams, S. M., & Goldman-Rakic, P. S. (1998). Widespread origin of the primate mesofrontal dopamine system. *Cerebral Cortex*, *8*, 321–345.

Young, R. R. (1984). Tremor in relation to certain other movement disorders. In L. J. Findley, & R. Capildeo (Eds.), *Tremor* (pp. 463–472). London, England: Macmillian Publishers Ltd.